Cerebral Cortex May 2015;25:1330–1347
doi:10.1093/cercor/bht326
Advance Access publication December 1, 2013

Hypocretin (Orexin) Regulates Glutamate Input to Fast-Spiking Interneurons in Layer V of the Fr2 Region of the Murine Prefrontal Cortex

Patrizia Aracri[1], Daniele Banfi[1], Maria Enrica Pasini[2], Alida Amadeo[2] and Andrea Becchetti[1]

[1]Department of Biotechnology and Biosciences, University of Milano-Bicocca, Milan 20126, Italy and [2]Department of Biomolecular Sciences and Biotechnology, University of Milano, Milan 20128, Italy

Address correspondence to Prof. Andrea Becchetti, Department of Biotechnology and Biosciences, University of Milano-Bicocca, piazza della Scienza, 2, Milan 20126, Italy. Email: andrea.becchetti@unimib.it

We studied the effect of hypocretin 1 (orexin A) in the frontal area 2 (Fr2) of the murine neocortex, implicated in the motivation-dependent goal-directed tasks. In layer V, hypocretin stimulated the spontaneous excitatory postsynaptic currents (EPSCs) on fast-spiking (FS) interneurons. The effect was accompanied by increased frequency of miniature EPSCs, indicating that hypocretin can target the glutamatergic terminals. Moreover, hypocretin stimulated the spontaneous inhibitory postsynaptic currents (IPSCs) on pyramidal neurons, with no effect on miniature IPSCs. This action was prevented by blocking 1) the ionotropic glutamatergic receptors; 2) the hypocretin receptor type 1 (HCRTR-1), with SB-334867. Finally, hypocretin increased the firing frequency in FS cells, and the effect was blocked when the ionotropic glutamate transmission was inhibited. Immunolocalization confirmed that HCRTR-1 is highly expressed in Fr2, particularly in layer V–VI. Conspicuous labeling was observed in pyramidal neuron somata and in VGLUT1+ glutamatergic terminals, but not in VGLUT2+ fibers (mainly thalamocortical afferents). The expression of HCRTR-1 in GABAergic structures was scarce. We conclude that 1) hypocretin regulates glutamate release in Fr2; 2) the effect presents a presynaptic component; 3) the peptide control of FS cells is indirect, and probably mediated by the regulation of glutamatergic input onto these cells.

Keywords: fast-spiking, HCRTR, OXR1, premotor, SB-334867, VGLUT

Introduction

Hypocretin 1 and 2 (de Lecea et al. 1998), also known as orexin A and B (Sakurai et al. 1998), are neuropeptides synthetized by neurons located in the lateral and posterior hypothalamus (Sakurai 2007). Initially implicated in feeding behavior, they were also found to regulate cortical arousal and the sleep-waking cycle. Hypocretin neurons discharge during active waking and stop firing during sleep (Lee et al. 2005; Mileykovskiy et al. 2005; Jones 2008). Their fibers innervate the arousal-controlling nuclei in brainstem, basal forebrain, and hypothalamus (Peyron et al. 1998; Hagan et al. 1999; Horvath et al. 1999; Bayer et al. 2001; Eggermann et al. 2001; Eriksson et al. 2001; Liu et al. 2002; Yamanaka et al. 2002). Disruption of the hypocretin system leads to narcolepsy with cataplexy in humans as well as in animal models (Chemelli et al. 1999; Lin et al. 1999; Peyron et al. 2000; Thannickal et al. 2000; Gerashchenko et al. 2003). Moreover, direct evidence that the activity of hypocretin cells regulates awakening was provided by specific photostimulation of these cells in the lateral hypothalamus (Adamantidis et al. 2007). Based on these and other evidences, hypocretins are now thought to exert a variety of physiological roles related to arousal, feeding, metabolic regulation, and the stress response (Sakurai et al. 1998; Sakurai 2007; Boutrel et al. 2010; Kukkonen 2013). A possible unifying view is that hypocretin neurons contribute to set the proper level of arousal necessary for exploratory and goal-oriented behaviors, in response to different physiological or psychological drives (Boutrel et al. 2010). In fact, narcoleptic patients display specific attention deficits related to the prefrontal executive functions that cannot be merely attributed to sleepiness (Rieger et al. 2003).

These notions have led to growing interest in the direct and indirect effects of hypocretins in the prefrontal cortex (PFC). The hypocretin-regulated basal forebrain and brainstem nuclei (Sutcliffe and de Lecea 2002) control the unspecific thalamocortical neurons located in the midline-intralaminar thalamic nuclei (Peyron et al. 1998; Bayer et al. 2002). These modulate attention and executive functions by targeting the apical dendrites of pyramidal neurons in PFC layers I and V (Lambe et al. 2007). However, hypocretin fibers also innervate the PFC (Peyron et al. 1998) and recent evidence indicates that hypocretins produce direct regulation of the mammalian PFC (Lambe and Aghajanian 2003; Lambe et al. 2005; Liu and Aghajanian 2008; Li et al. 2010), where such innervation is much denser than in other neocortical areas (Fadel and Deutch 2002).

Irrespective of the brain region, the cellular effect of hypocretin is generally excitatory (Hagan et al. 1999; Yamanaka et al. 2002; Lambe and Aghajanian 2003; Bayer et al. 2004; Lambe et al. 2005) and is mediated by 2 G-protein coupled receptors, HCRTR-1 and HCRTR-2 (Sakurai et al. 1998). HCRTR-1 binds more potently hypocretin 1 whereas HCRTR-2 poorly discriminates between the 2 peptides (Holmqvist et al. 2001; Ammoun et al. 2003). Activation of both receptors can elevate cytosolic Ca^{2+} by multiple mechanisms (Smart et al. 1999; Kane et al. 2000; Eriksson et al. 2001; Kohlmeier et al. 2008), but inhibition of K^+ channels (Bayer et al. 2002, 2004; Beuckmann and Yanagisawa 2002; Xia et al. 2005) and hyperpolarization-activated HCN channels (Li et al. 2010) have also been reported.

In rat brain, these receptors have a widespread and partly overlapping pattern of expression (Hervieu et al. 2001; Marcus et al. 2001). In the PFC, their expression is complementary, with HCRTR-1 being preferentially expressed in layers III/V and HCRTR-2 in layers II/VI (Marcus et al. 2001). In the mouse, evidence is fragmentary. Conspicuous expression of HCRTR-1 was recently observed in layer V of the prelimbic PFC, where stimulation with hypocretin 1 produces excitation of pyramidal neurons (Li et al. 2010). However, the different PFC regions are increasingly recognized to be morphologically and functionally heterogeneous (Franklin and Chudasama 2011). In fact, the hypocretin stimulus of glutamate release in the rat medial PFC is

not observed in the parietal cortex (Lambe and Aghajanian 2003). Virtually nothing is known about the physiology of hypocretins in other associative cortices. Because these peptides regulate the reward-driven goal-oriented behavior, we focused on the dorsomedial shoulder of the murine PFC (Fig. 1*D*). This region is also known as secondary motor area (M2; Franklin and Chudasama 2011), medial precentral region (Hoover and Vertes 2007; Kargo et al. 2007), or frontal area 2 (Fr2; Heidbreder and Groenewegen 2003; Uylings et al. 2003; Palomero-Gallagher and Zilles 2004). Fr2 displays features related to the human dorsolateral PFC, with partial overlap with higher association functions (Uylings et al. 2003). It also presents peculiar connectivity, as it is innervated by both sensory and parietal regions of the cortex and projects to the motor cortex and dorsolateral striatum (Berendsee et al. 1992; Condé et al. 1995). Therefore, Fr2 is probably implicated in producing the appropriate behavioral response to situations that require immediate attention (Hoover and Vertes 2007). Furthermore, recent work in mice shows that Fr2 neurons are important substrates of the decision–execution steps that mediate the motivation-dependent goal-oriented tasks (Kargo et al. 2007). Hence, Fr2 seems a particularly relevant target of the arousal/attentive effects of hypocretins.

We studied the effects of hypocretin 1 on glutamate and GABA release in layer V, the main subcortically projecting layer (Richardson et al. 2007). Although the overall network activity depends on the balance of the excitatory and inhibitory actions, whether and how hypocretin regulates GABAergic transmission in the neocortex is unknown. We thus gave special attention to the regulation of fast-spiking (FS) interneurons, which represent the majority of neocortical basket cells (Rudy et al. 2011). We coupled electrophysiological experiments with immunocytochemical determinations of the HCRTR-1 distribution in the glutamatergic and GABAergic elements. In particular, the glutamatergic fibers were distinguished by marking the vesicular glutamate transporters VGLUT1 and VGLUT2. Because the latter is almost exclusively expressed in the extrinsic glutamatergic fibers, comparing the distribution of VGLUT1 and VGLUT2 indicates the balance of intracortical and extrinsic (mostly thalamocortical) glutamatergic fibers (Hur and Zaborsky 2005; Nakamura et al. 2005; Graziano et al. 2008). Our results show that hypocretins regulate synaptic transmission in the Fr2 prefrontal region, and suggest that the direct regulatory actions of hypocretins in premotor regions are much more prominent than previously thought.

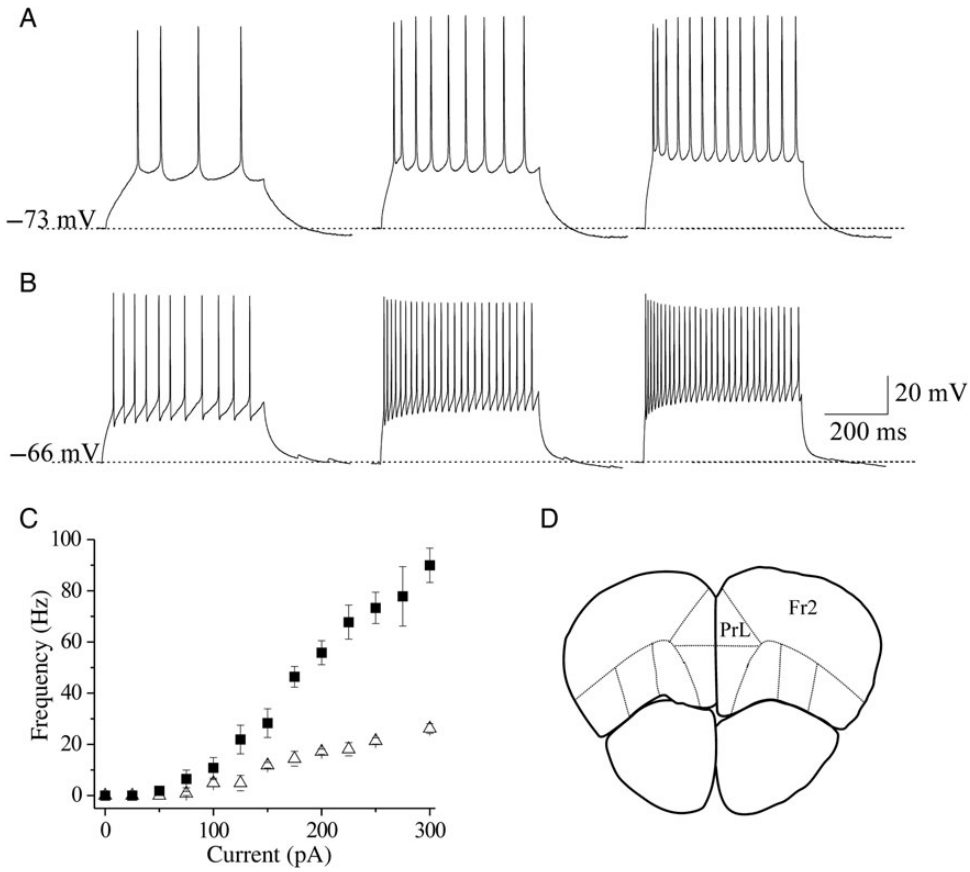

Figure 1. Identification of pyramidal and FS cells in Fr2 layer V. (*A*) Regular spiking pyramidal cells were characterized by testing the firing response to consecutive depolarizing current steps, lasting 500 ms. The responses to above-threshold current steps (from left to right: 100, 200, and 300 pA) are shown for a representative neuron, showing the classical low-frequency firing with adaptation. (*B*) A similar procedure was applied to select FS cells. This neuron exhibited the high-frequency spiking typical of FS interneurons, with little adaptation. (*C*) Relation between injected current and firing frequency for regular spiking pyramidal cells (triangles; $n = 11$) and FS cells (squares; $n = 14$). Data points are average firing frequencies calculated from an ensemble of similar neurons, and plotted as a function of injected current. (*D*) A sketch is shown of a coronal murine brain section, in which the continuous lines mark the main functional regions typically recognized in the PFC. PrL, prelimbic region; Fr2, frontal area 2. Sections such as these were generally cut in the region between +2.68 and +2.10 mm from bregma.

Materials and Methods

Experiments were carried out according to the Principles of Laboratory Animal Care (directive 86/609/EEC) on FVB mice (Harlan, San Pietro al Natisone, Italy). All efforts were made to minimize the number of animals used. Unless otherwise indicated, chemicals and drugs were purchased from Sigma-Aldrich, Italy. The source of antibodies is always indicated explicitly.

Selected Neocortical Areas

To study the Fr2 region of the PFC, we cut coronal sections between +2.68 and +2.10 mm from bregma (according to Paxinos and Franklin 2001; Fig. 1*D*). For details about the nomenclature of this region, see Aracri et al. (2013). For somatosensory cortex (SS), sections were selected between +0.50 and +0.02 mm from bregma (primary SS cortex).

Brain Slice Preparation for Electrophysiology

Mice, aged 17–30 days, were deeply anesthetized with ethyl ether and decapitated. Brains were removed and placed in ice-cold solution containing (mM): 87 NaCl, 21 $NaHCO_3$, 1.25 NaH_2PO_4, 7 $MgCl_2$, 0.5 $CaCl_2$, 2.5 KCl, 25 D-glucose, and 75 sucrose, aerated with 95% O_2 and 5% CO_2 (pH 7.4). Coronal slices (300 μm thick) were cut with a VT 1000S vibratome (Leica Microsystems, Mannheim, Germany) and incubated at 32 °C for at least 1 h, in the same solution as above, before being transferred to the recording chamber.

Whole-Cell Recordings

Neurons were voltage- or current-clamped with a Multiclamp 700A patch-clamp amplifier (Molecular Devices, Union City, CA, USA), at 32 °C. Low-resistance micropipettes (2–3 MΩ) were pulled from borosilicate capillaries with a P-97 Flaming/Brown Micropipette Puller (Sutter Instrument Company, Novato, CA, USA). The cell capacitance and series resistance (up to 75%) were always compensated. Experiments in which series resistance did not remain below 10 MΩ (tipically 5–8 MΩ) were discarded. Input resistance was generally close to 100 MΩ. Synaptic currents were low-pass filtered at 2 kHz and digitized at 5 kHz, with pClamp9/Digidata 1322A (Molecular Devices).

When recording, slices were perfused at 1.8 mL/min with artificial cerebrospinal fluid (ACSF), containing (mM): 135 NaCl, 21 $NaHCO_3$, 0.6 $CaCl_2$, 3 KCl, 1.25 NaH_2PO_4, 1.8 $MgSO_4$, and 10 D-glucose, aerated with 95% O_2 and 5% CO_2 (pH 7.4). Cells were examined with an Eclipse E600FN microscope (Nikon Instruments, Sesto Fiorentino, Italy), equipped with a water immersion differential interference contrast objective and an infrared CCD 100 camera (DAGE-MTI, Inc., Michigan City, IN, USA). For EPSC recordings, pipette contained (mM): 135 K gluconate, 5 KCl, 2 $MgCl_2$, 10 HEPES, 2 MgATP (pH 7.2). Resting membrane potential (V_{rest}) was measured in open circuit mode, soon after obtaining the whole-cell configuration. The membrane potential (V_m) values given in the text were not corrected for liquid junction potentials. When recording the IPSCs at +10 mV, pipette contained (mM): 140 Cs gluconate, 2 $MgCl_2$, 10 HEPES, 2 MgATP (pH 7.2). In this case, Cs^+ was used to inhibit the voltage-gated K^+ currents (Aracri et al. 2010). Agonists and antagonists were applied through our perfusion solution and their effects calculated at the steady state, which was usually reached within 2–3 min. Experiments in which the average frequency of synaptic events after washout was <75% of the value measured before treatment were discarded.

Drugs

Stock solutions of hypocretin 1 (100 μM), tetrodotoxin (TTX; 1 mM; Tocris Bioscience, UK), D(–)-2-amino-5-phosphono-pentanoic acid (AP5; 100 mM) and $CdCl_2$ (50 mM) were prepared in distilled water. Stock solutions of 6-cyano-7-nitroquinoxaline-2,3-dione (CNQX; 20 mM) and SB-3348671 (1 mM) were prepared in dimethyl sulfoxide. Aliquots were stored at −20 °C. All drugs were dissolved daily at the final concentration in ACSF.

Immunoblot Analysis

Mice were anesthetized with diethyl ether and decapitated. The brain was quickly removed and the Fr2 and SS cortices were separated with fine jeweller's forceps under a binocular microscope and frozen at –80 °C until use. When needed, this tissue was washed 3 times with 50 mM Tris-buffered saline (TBS) and then homogenized with a Teflon-on-glass homogenizer in TBS supplemented with a general-purpose protease inhibitor cocktail (Mini Protease Inhibitor Mixture, Roche Applied Science). Homogenates were centrifuged at 1000 × *g* for 5 min at 4 °C. Next, the membrane proteins were separated from the intracellular proteins by resuspending the pellets according to the Mem-PER(r) Eukaryotic Membrane Protein Extraction Reagent Kit (Pierce Biotechnology, Rockford, IL, USA). Proteins were quantified by the Bradford method, using the AppliChem solution. Samples containing 50 mg of total proteins were heated to 100 °C for 5 min in sample buffer (0.6 g/100 mL Tris, 2 g/100 mL SDS, 10% glycerol, 1% β-mercaptoethanol, pH 6.8, 0.03% bromophenol blue), loaded onto 10% SDS–PAGE gel and run at 60 mA until the dye front reached the bottom of the gel, after which they were electrotransferred to nitrocellulose membranes (Mini Trans-blot, Bio-Rad Laboratories, Hercules, CA, USA) in 20% methanol/25 mM Tris/192 mM glycine at 70 V, for 2 h at room temperature. Nitrocellulose membranes were treated with a blocking solution containing 5% nonfat dry milk in TBS supplemented with 0.1% (v/v) Tween 20 (TBST) for 2 h at room temperature, to block aspecific protein binding sites. They were then incubated overnight at 4 °C with a goat polyclonal anti-HCRTR1 (OriGene Technologies, Rockville, MD, USA; 1:500) primary antibody diluted in blocking solution. The following day, membranes were extensively washed with TBST buffer and incubated for 1 h with a secondary antibody horse anti-goat biotin conjugated (Vector, 1:10 000) at room temperature. The immunoreactive regions were detected by alkaline phosphatase-conjugated streptavidin (Streptavidin-AP, Vector; 1:2000) at room temperature for 2 h; washed twice in TTBS and once in TBS, and finally developed in AP substrate: 100 mM Tris–HCl, 100 mM NaCl, 5 mM $MgCl_2$, 150 μg/mL 5-bromo-4-chloro-3-indolyl phosphate (BCIP), 30 μg/mL nitroblue tetrazolium (NBT), pH 9.5. The same membranes were reblotted with monoclonal anti-α-tubulin (Sigma; 1:1000) as a loading control. To this purpose, primary and secondary antibodies were removed from the membrane by incubation for 15 min at 37 °C in Restore Western Blotting stripping buffer (Pierce Biotechnology, Inc.). Membranes were then washed twice with TBST, and processed with primary and secondary (horse anti-mouse biotin conjugated, Vector; 1:10 000) antibodies. Band intensities were quantified by densitometric analysis (NIH ImageJ software) on scanned films. Immunoreactivity with anti-HCRTR1 was normalized to the one obtained with anti-α-tubulin. The following negative controls were carried out: 1) omission of anti-HCRTR1; 2) preadsorption of the antiserum with the corresponding 5 mM synthetic peptide for 12 h at 4 °C, before use.

Cortical Tissue Preparation for Immunocytochemistry

Mice, aged 21–40 days, were anesthetized with intraperitoneal 4% chloral hydrate (2 mg/100 g) and sacrificed by intracardiac perfusion of 4% paraformaldehyde, in phosphate buffer 0.1 M (pH 7.2–7.4). Brains were removed and incubated in the same solution, at 4 °C for 2 h. Coronal sections (50 μm thick) were cut with a VT1000S vibratome (Leica Microsystems). Some sections (e.g., Fig. 1) were stained with thionin (Nissl method) for cytoarchitecture analysis, by using standard procedures (Franklin and Chudasama 2011). At least 3 sections for each examined cortical area (Fr2 and SS) were selected from each perfused brain to examine HCRTR-1 expression and colocalization with GABAergic and glutamatergic markers, by immunofluorescence.

Confocal Microscopy

Sections were mildly permeabilized with ethanol (10%, 25%, 10%, 5 min each), instead of Triton X-100, to increase the immunoreagent penetration. Subsequently, they were pretreated with PBS containing 1% bovine serum albumin for 30 min, and incubated overnight in a mixture of 2 or 3 primary antibodies. Finally, a 2-h incubation was carried out in a mixture of the appropriate secondary antibodies, at room temperature. Images were analyzed with a TCS SP2 AOBS

laser scanning confocal microscope (Leica Microsystems). For control of anti-HCRTR-1 antibody, preabsorption assays were performed with the corresponding blocking peptide, with sequence C-YNFLSGKFREQFK, from the internal region of the protein (Origene). Brain sections were treated with anti-HCRTR-1, previously incubated (for 12–24 h at 4 °C, with mild agitation) with the specific peptide it recognizes (3- to 5-fold molar excess of synthetic peptide, relative to IgG concentration at the normal antibody dilution). No signal was detected after preabsorption.

Primary Antibodies

Anti-HCRTR-1: polyclonal, made in goat, diluted at 1/150 (Origene); anti-parvalbumin (PV): polyclonal, made in rabbit, 1/1500 (Swant, Bellinzona, Switzerland); anti-glutamic acid decarboxylase, 65 kDa form (GAD65): monoclonal, made in mouse, diluted at 1/300 (Chemicon); anti-vescicular glutamate transporters type 1 (VGLUT1): polyclonal, made in rabbit, diluted at 1/600 (Synaptic System); antivesicular glutamate transporters type 2 (VGLUT2): polyclonal, made in rabbit, diluted at 1/500 (Synaptic System). The specificity of primary antibodies were assessed by negative controls, that is, omission of the primary antiserum and preabsorption of the primary antiserum with the corresponding synthetic peptide, when available (see above for anti-HCRTR-1; for anti-VGLUT1 and anti-VGLUT2, see Aracri et al. 2013).

Secondary Antibodies

For anti-HCRTR1: donkey anti-goat RedX (DAG-RedX; Jackson ImmunoResearch) diluted at 1/200. For VGLUT1 and VGLUT2: Cy2-conjugated donkey anti-rabbit (DAR-Cy2; Jackson ImmunoResearch) diluted at 1/200. For PV: Cy2-conjugated donkey anti-rabbit (DAR-Cy2; Jackson ImmunoResearch) diluted at 1/200 or Cy5-conjugated donkey anti-rabbit (DAR-Cy5, blue signal; Jackson ImmunoResearch) diluted at 1/400. For the monoclonal GAD65: biotinylated horse anti-mouse (bHAM; Vector, Inc.) diluted at 1/200, and Alexa-488 labeled streptavidin (1/200, Molecular Probes).

Analysis of Synaptic Events

Experimental traces for IPSCs, EPSCs, and action potential firing were analyzed offline with Clampfit 9.2 (Molecular Devices), Mini Analysis Software 6.0.7 (Synaptosoft, GA, USA), and OriginPro 8 (OriginLab, MA, USA) software. The IPSCs included both smoothly shaped isolated signals with a peak amplitude larger than 40 pA and composite signals. Events were inspected one by one and those not presenting the typical shape of synaptic currents were rejected. The baseline noise (peak to peak) was about 5 pA. The detection threshold was generally set at 7–8 pA. A similar procedure was applied to EPSCs. For each cell, the statistical comparison of the cumulative distributions of IPSC or EPSC amplitudes and interevent intervals in the different experimental conditions was conducted with the Kolmogorov–Smirnov (KS) method. The analysis was carried out on at least 2-min continuous recording at the steady state. The number of synaptic current events occurring in this time span depended on experimental conditions, but was generally higher than 500 and usually around 1500. The excitatory postsynaptic potential (EPSP) events related to Figure 7 were detected by setting a threshold at 4 times the root mean square noise (around 0.5 mV) of the V_{rest} trace. This was calculated in a time span of at least 10 s devoid of synaptic events (e.g., Kiritoshi et al. 2013).

Statistical Comparison of Populations of Experiments

The average results obtained in several cells are given as mean values ± standard error of the mean (SEM). The number of experiments (n) refers to the number of neurons sampled in different brain slices, prepared from at least 3–4 mice. In this case, statistical significance was assessed with paired Student's t-test, which assumes that the differences are sampled from a Gaussian distribution. This assumption was systematically tested with the KS method. The level of significance was set to $P = 0.05$. Lack of statistical significance is indicated by NS. Immunoblot data are also reported as mean values ± SEM and significance was tested with paired t-test.

Results

Patch-clamp recordings were carried out in Fr2 layer V. To reveal the global neuropeptide effect, we applied hypocretin 1, which effectively stimulates both HCRTR-1 and HCRTR-2, at the concentrations we used (100–500 nM; Ohno and Sakurai 2008).

Distinction of FS Interneurons and Regular Spiking Pyramidal Cells

Several populations of interneurons have been identified in rodent neocortex, whose functional role is debated (e.g., Kawaguchi and Kubota 1997; Couey et al. 2007; Kubota et al. 2011). Here, we focus on FS interneurons and regular spiking excitatory cells, which are well distinguished by their firing pattern (Connors and Gutnick 1990). In mouse neocortex, FS cells exhibit morphological and physiological properties analogous to those observed in the rat. In layer V, FS neurons likely constitute the majority of basket cells, the predominant interneuron type in this layer (Kawaguchi and Kubota 1997; Kawaguchi and Kondo 2002; Gonchar et al. 2008). After localizing the putative FS cells by shape and laminar location, their firing pattern was tested by applying depolarizing current steps (Fig. 1*B*). Below threshold, cells exhibited a quasi-linear response whereas, above threshold, they showed the typical nonadapting high-frequency firing (Couey et al. 2007; Trantham-Davidson et al. 2008). Figure 1*C* (squares) shows the relation between injected current and firing frequency in a representative sample. These results are consistent with literature on FS cells (e.g., Bacci et al. 2003). The V_{rest} of the FS cells pooled in Figure 1*C* was −65.4 ± 0.8 mV ($n = 14$).

The regular spiking pyramidal cells were recognized as previously reported (Aracri et al. 2010). When tested with depolarizing current pulses, they displayed the typical low-frequency action potential firing with adaptation (Connors and Gutnick 1990; Porter et al. 1999). A typical example is shown in Figure 1*A*. The corresponding stimulus-firing relationship for a representative sample of cells is shown in Figure 1*C* (triangles). The V_{rest} of these neurons was generally around −70 mV. In particular, the pyramidal cells pooled in Figure 2*C* had $V_{rest} = -70.9 \pm 0.59$ mV ($n = 11$).

Hypocretin Increased the Spontaneous EPSC Frequency, in FS Cells

We first studied whether hypocretin affected glutamate release onto FS interneurons, by measuring the spontaneous EPSCs (sEPSCs). These were recorded at −70 mV, which is close to the reversal potential of GABAergic IPSCs (Aracri et al. 2010). Typical current traces are shown in Figure 2*A*. Application of AP5 (50 μM) and CNQX (10 μM), which block, respectively NMDA (*N*-methyl-D-aspartate) and AMPA [(*R*,*S*)-α-amino-3-hydroxy-5-methyl-4-isoxazole propionic acid] ionotropic glutamate receptors, generally abolished these currents (not shown). Subsequent perfusion with 100 nM hypocretin 1 increased the sEPSC frequency, as is shown by comparing the cumulative distributions of interevent intervals (Fig. 2*B*) with the corresponding control. Distributions were computed from 2-min continuous recordings, in the absence or in the presence of the peptide. No significant effect was produced on the

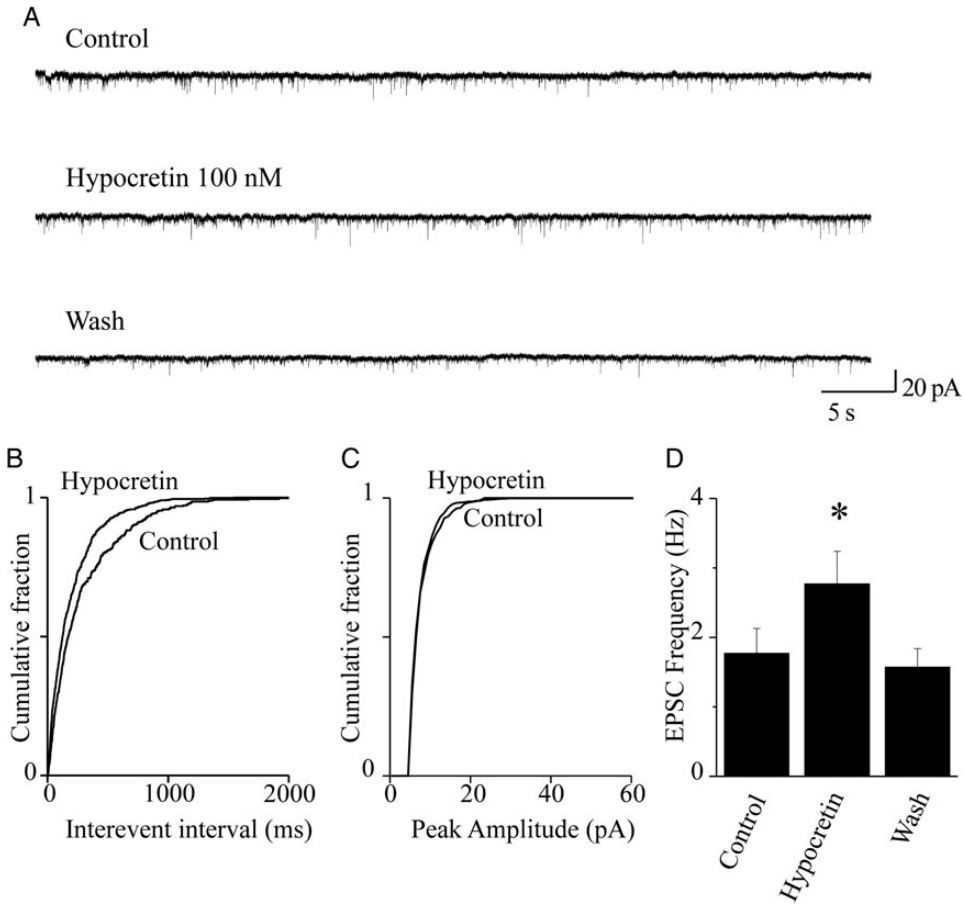

Figure 2. Hypocretin 1 stimulates glutamate release onto FS neurons. (*A*) Spontaneous EPSCs were recorded from FS neurons at −70 mV. Current traces represent 60-s continuous recording, before (Control), during (Hypocretin 100 nM), and after (Wash) peptide application. Hypocretin increased EPSC frequency, in a reversible way. (*B*) Cumulative distribution of the EPSC interevent intervals, calculated from the same experiment as in (*A*), in the presence or absence of hypocretin, as indicated. The peptide significantly decreased the interevent intervals ($P < 0.01$, with KS test). (*C*) Cumulative distribution of the EPSC amplitudes, in the presence or absence of hypocretin, in the same neuron. The peptide produced no significant alteration of the EPSC amplitudes (NS with KS test). (*D*) Hypocretin 1 produced a significant stimulatory effect in 7 of 8 neurons tested. Bars give the average EPSC frequency calculated from these cells. The plotted values were calculated from 2-min continuous recording in the indicated conditions, at the steady state. On average, the neuropeptide produced an ∼60% increase in EPSC frequency (*$0.01 < P < 0.05$; comparison between hypocretin and control).

current amplitudes (Fig. 2*C*). The results of a series of such experiments are summarized in Figure 2*D*, which gives the average increase of sEPSC frequency produced by hypocretin in 7 similar experiments. On average, hypocretin brought the sEPSC frequency from 1.77 ± 0.36 to 2.77 ± 0.47 Hz ($P < 0.05$; $n = 7$). The effect was fully reversible, as the average sEPSC frequency after 2 min of hypocretin removal was 1.57 ± 0.27 Hz (NS compared with the initial control; $n = 7$). We conclude that hypocretin 1 stimulates glutamate release onto FS cells, in Fr2 layer V.

Hypocretin Increased the Frequency of Miniature EPSC, in FS Cells

The sEPSCs contain action potential-dependent and action potential-independent (miniature) synaptic events. To distinguish the contribution of these 2 types of events, we measured miniature EPSC (mEPSC) in the presence of 1 μM TTX, to block the action potential-dependent glutamate release (Fig. 3). Application of TTX alone has been previously shown to be sufficient to block the firing-dependent release in the rat neocortex (e.g., Lambe and Aghajanian 2003). An alternative procedure to isolate the miniature events is to apply TTX plus Cd^{2+}, to also block L-type calcium channels (Aracri et al. 2010). The 2 procedures had similar efficacy, in our preparation. Hence, we show results obtained with no Cd^{2+} added, which could mask a possible effect of hypocretin on G protein-dependent presynaptic Ca^{2+} channels (Spinazzi et al. 2006). This point is further discussed later, when the effectiveness of the 2 procedures is compared for IPSCs (Fig. 6). Experiments and data analysis were as illustrated in Figure 2, except for the presence of TTX. Figure 3*A* illustrates the EPSC traces measured in the indicated conditions during a typical experiment. TTX produced the expected decrease in sEPSC frequency and amplitude. The subsequent application of 100 nM hypocretin 1 significantly increased the mEPSC frequency, with no significant effect on the events' amplitude (not shown). The cumulative distribution of the interevent intervals for this experiment is shown in Figure 3*B*. The overall results are summarized in Figure 3*C*, which plots the average EPSC frequency calculated from 6 experiments, in the indicated conditions. Hypocretin brought the mEPSC frequency from 5.8 ± 1.89 to 8.62 ± 2.6 ($P < 0.05$; $n = 6$). The effect was reversible, as after washout the mEPSC frequency was 4.48 ± 1.55 (NS compared with the value measured before application of

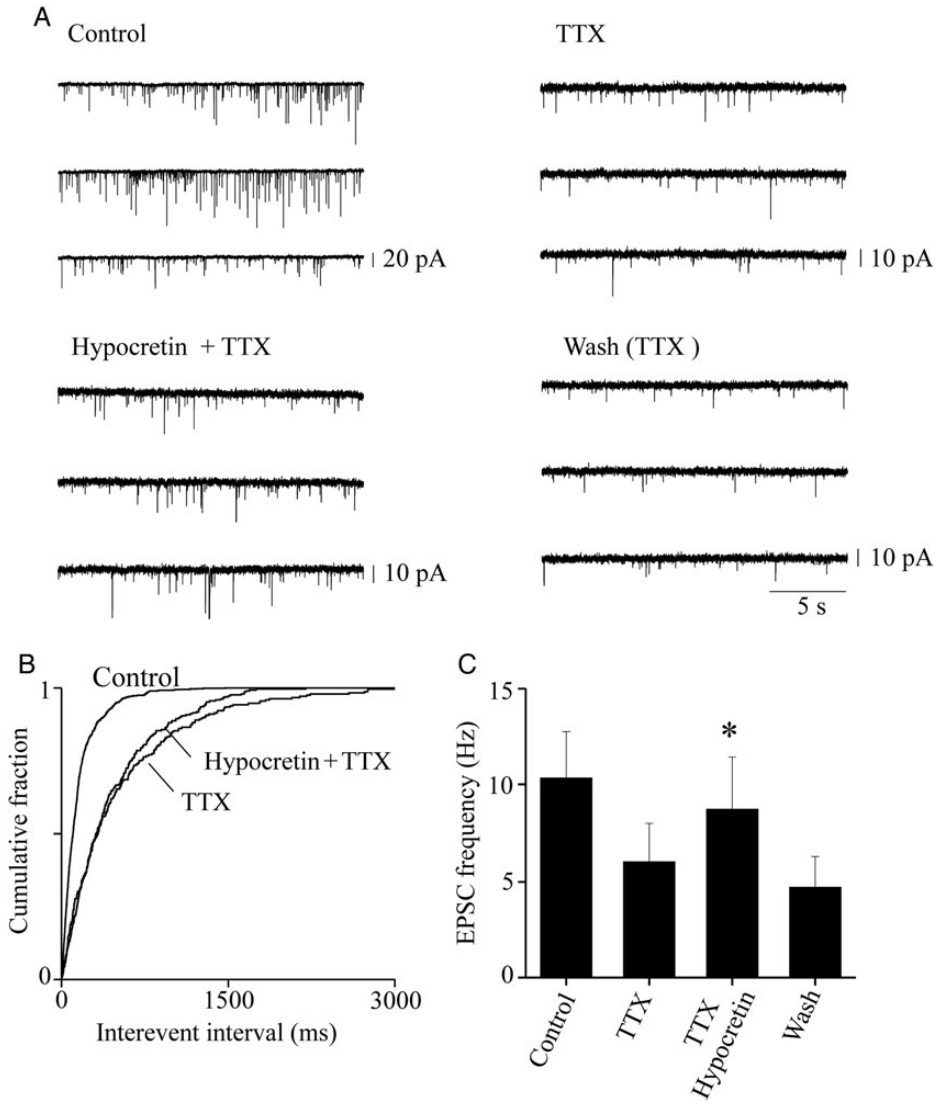

Figure 3. Presynaptic effect of hypocretin on glutamatergic terminals. (*A*) Sample EPSC traces recorded at −70 mV from a typical FS cell, during continuous recording in the indicated conditions. Application of 0.5 μM TTX produced the expected decrease of the EPSC amplitudes and frequency, thus revealing the miniature events. The mEPSC frequency was stimulated by 100 nM hypocretin 1, and the effect was reversible on washout. (*B*) Cumulative distribution of the EPSC interevent intervals in the same experiment, calculated from 2-min continuous recording in the indicated conditions. The frequency of the mEPSCs revealed by TTX was increased by hypocretin ($P < 0.01$, with KS test). (*C*) Similar results were obtained in 6 analogous experiments. In these experiments, mice were aged 25–30 days, to maximize the basal synaptic activity and thus avoid the risk of having too few miniature events for our analysis. To increase the number of miniature events in the presence of TTX, and thus Bars give the average mEPSC frequency, calculated for 2 min of continuous recording at the steady state, in the indicated conditions. Hypocretin produced an ∼50% increase in the average mEPSC frequency (*$0.01 < P < 0.05$; comparison between hypocretin+TTX and TTX). Full statistics are given in the main text.

the peptide). These results suggest that hypocretin can target the glutamatergic terminals, in murine Fr2 layer V.

Hypocretin Increases the Spontaneous IPSC Frequency, in Layer V Pyramidal Neurons

In the neocortex, pyramidal neuron firing is tightly controlled by the surrounding basket cells (Fig. 7*C*), whose action is particularly effective in layer V (Douglas and Martin 2004). Therefore, we studied the effect of hypocretin on GABA release. To this purpose, we measured the spontaneous IPSCs (sIPSCs) in pyramidal neurons, in the presence or absence of the peptide. Figure 4*A* shows typical sIPSC traces recorded at +10 mV. At this V_m, the IPSC amplitude is maximized, whereas the EPSCs are minimized (Aracri et al. 2010). Slices were perfused with 100 nM hypocretin 1, for 4 min. Treatment significantly increased the sIPSC frequency and amplitude. All synaptic events were abolished by 10 μM bicuculline, which demonstrates their GABAergic nature (not shown). The cumulative distributions of the interevent intervals (Fig. 4*B*) for 2-min continuous recording at the steady state, were statistically tested with a KS test, as detailed in the figure legend. Similar results were obtained in 7 experiments. On average (Fig. 4*D*), the sIPSC frequency was brought by hypocretin from 8.0 ± 1.1 to 9.2 ± 1.2 Hz ($n = 7$; $P < 0.001$). The effect on sIPSC frequency was accompanied by an increase of sIPSC amplitude, as is clear from both the current traces and the cumulative distribution of current amplitudes (Fig. 4*C*). These data indicate that hypocretin can regulate GABA release onto regular spiking pyramidal cells, in Fr2 layer V.

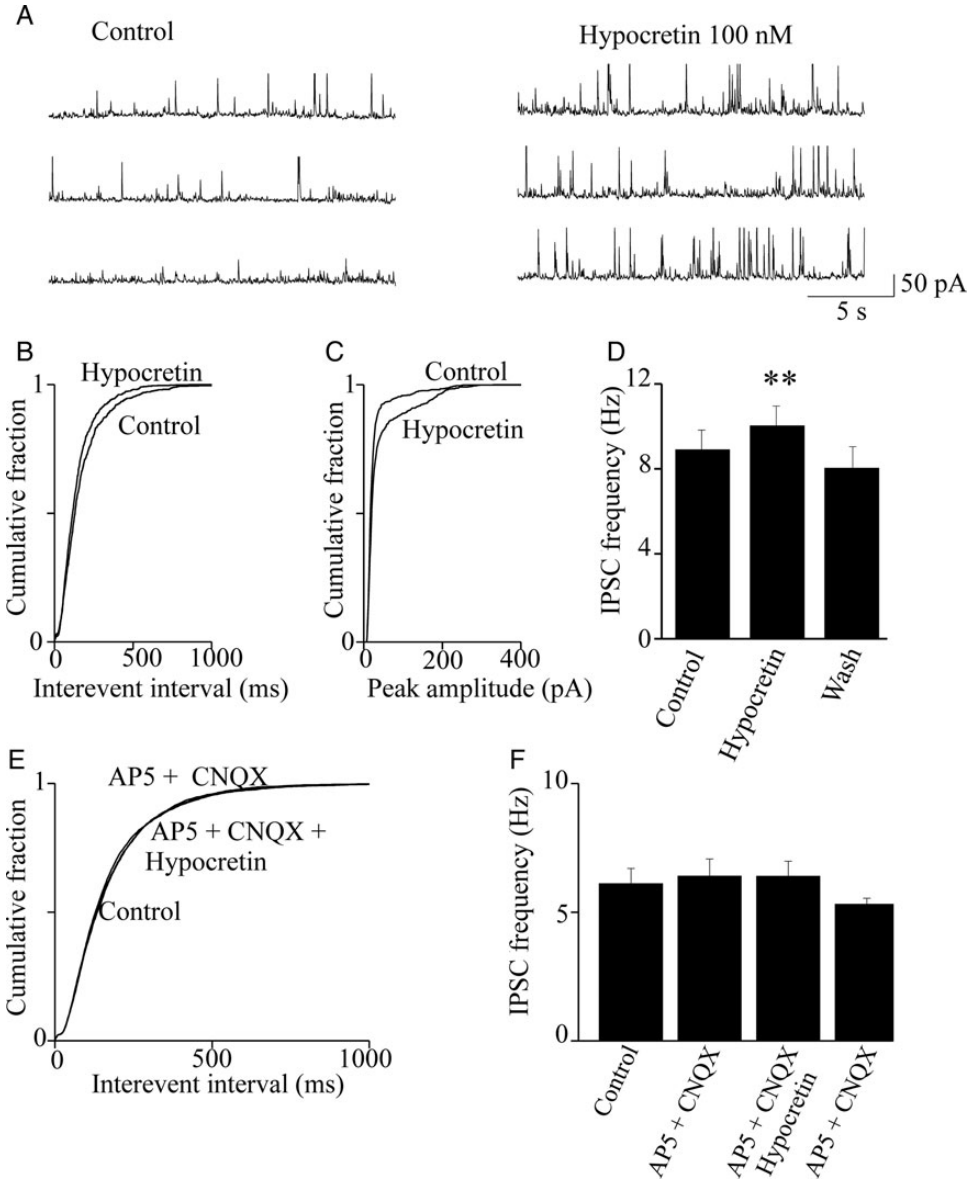

Figure 4. Hypocretin stimulates spontaneous IPSCs in pyramidal neurons. (*A*) IPSC traces recorded from a typical pyramidal neurons at +10 mV. The IPSC frequency was increased by hypocretin 1 (100 nM) and abolished by bicuculline (10 μM; not shown). (*B*) Cumulative distribution of the interevent intervals calculated from the same experiment. Hypocretin significantly increased the event frequency ($P < 0.01$, with KS test). (*C*) In this experiment, hypocretin also increased the average IPSC amplitude, as is illustrated by the cumulative distribution of amplitudes in the presence and absence of hypocretin ($P < 0.01$, with KS test). (*D*) Similar results were obtained in 7 of 9 experiments. Bars give the average IPSC frequency in control condition, in the presence of hypocretin and after washout, as indicated. Bar values were calculated from 2-min continuous recording, at the steady state. Hypocretin produced an average increase of IPSC frequency of ~15% (**$P < 0.01$; comparison between hypocretin and control). Full statistics are given in the main text. (*E*) Cumulative distribution of the spontaneous IPSC interevent intervals in a representative experiment, calculated in control condition, in the presence of 50 μM AP5 and 10 μM CNQX (AP5 + CNQX) and in the presence of AP5, CNQX, and hypocretin (AP5 + CNQX + Hypocretin). No significant difference was observed between treatments, as tested in each cell by the KS test. (*F*) Similar results were obtained in 7 experiments. Bars give the average IPSC frequency, in the indicated conditions. Data analysis was as in (*D*). No differences were observed between treatments (statistics are given in the main text).

Hypocretin is Ineffective on GABA Release When Ionotropic Glutamate Receptors are Blocked

Because hypocretin stimulates the glutamatergic input on FS cells (Figs 2 and 3), a possible explanation of the data shown in Figure 4*A–D* is that hypocretin stimulates the glutamatergic drive onto FS cells, which in turn stimulates GABA release onto pyramidal cells. If this hypothesis is correct, the stimulatory effect of hypocretin on GABA release should be abolished by inhibiting the excitatory drive on interneurons. Hence, we tested the effect of hypocretin 1 on the pyramidal cell sIPSCs, after blocking the ionotropic glutamate receptors with 50 μM AP5 and 10 μM CNQX. Under these conditions, hypocretin was completely ineffective. As is shown in Figure 4*E* for a typical experiment, the cumulative distributions of the interevent intervals in control condition, in the presence of AP5 plus CNQX and in the presence of AP5, CNQX, and hypocretin were virtually indistinguishable. The results obtained in 7 similar experiments are summarized in Figure 4*F*. The average sIPSC frequency was 6.42 ± 0.67 Hz, in the presence of AP5 plus CNQX, and 6.40 ± 0.58 Hz, in the presence of AP5, CNQX, and hypocretin (NS; $n = 7$). These results suggest that the hypocretin-dependent stimulation of

GABA release onto pyramidal cells requires intact glutamatergic transmission.

The Hypocretin Effect on IPSCs is Mediated by HCRTR-1

We next tested whether the above effect was caused by specific peptide interaction with one of its receptors. The hypocretin-dependent increase of sIPSCs was prevented by 2 min pretreatment with 1 μM SB-334867, a specific inhibitor of HCRTR-1 (Smart et al. 2001). Typical current traces are illustrated in Figure 5*A*. The cumulative distribution of interevent intervals in the presence of SB-334867 alone and SB-334867 plus hypocretin were almost superimposable (Fig. 5*B*). Similar results were obtained in 7 experiments. On average (Fig. 5*C*), the sIPSC frequency in presence of SB-334867 (7.05 ± 1.05 Hz) was not significantly different from that calculated in presence of SB-334867 plus orexin (5.97 ± 0.72 Hz; $n = 7$). We conclude that the stimulation produced by hypocretin 1 on GABA release onto layer V pyramidal cells mainly depends on activation of HCRTR-1, in our preparation.

Hypocretin 1 Does not Affect the Miniature IPSC Frequency, in Layer V Pyramidal Neurons

The results shown in Figure 4 do not rule out that hypocretin also produces direct regulation of the GABAergic terminals. To test this hypothesis, we measured miniature IPSC (mIPSCs) on pyramidal neurons. Once again, we compared the effects of revealing the mIPSCs with either 0.5 μM TTX, or 0.5 μM TTX plus 50 μM Cd^{2+}. A representative experiment is illustrated in Figure 6*A*. Treatment with TTX and Cd^{2+} strongly decreased the frequency and amplitude of IPSCs, as expected. The effect

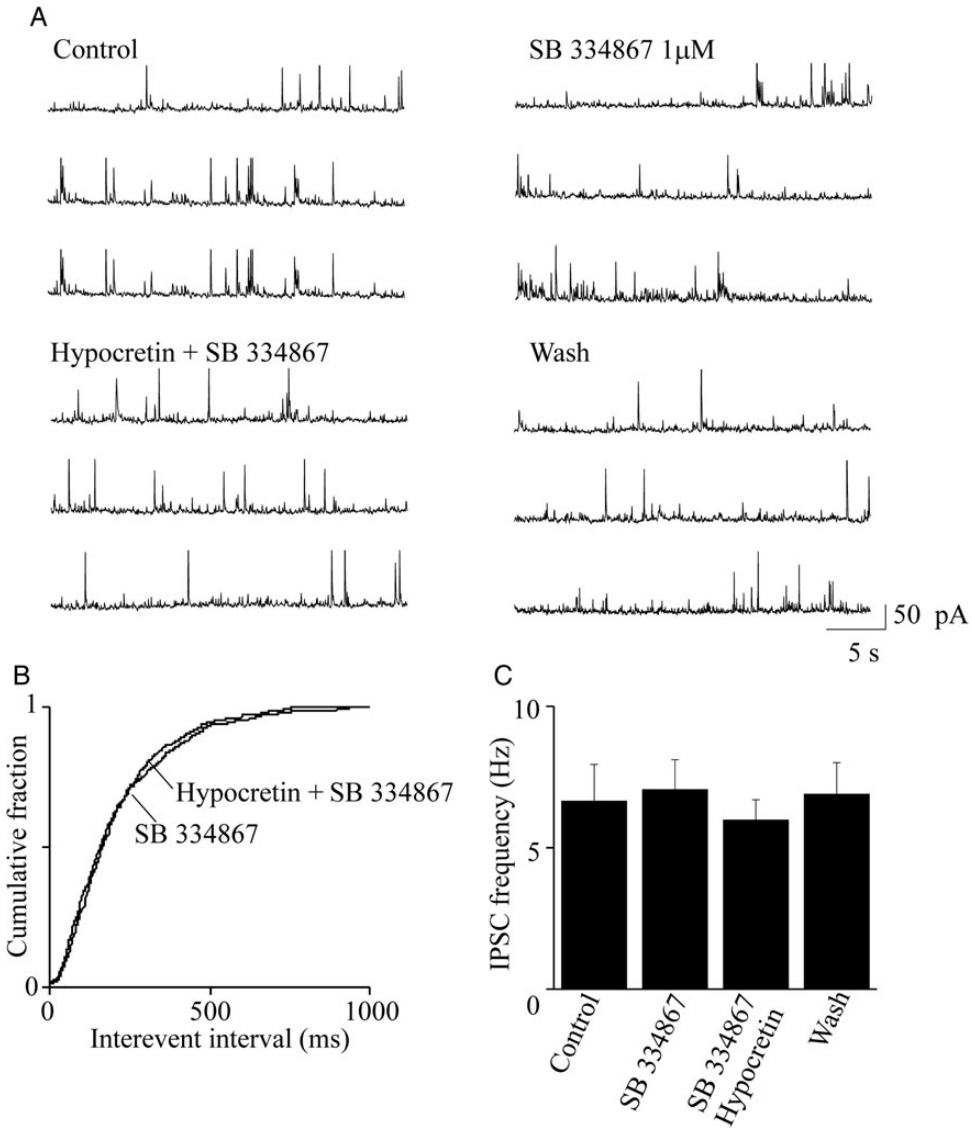

Figure 5. Blocking HCRTR-1 inhibits the hypocretin-dependent stimulus of spontaneous IPSCs. (*A*) Representative spontaneous IPSCs recorded from a pyramidal neuron at +10 mV, in the indicated conditions. The effect of 1 μM SB 3 348 671 was tested in the absence and in the presence of 100 nM hypocretin 1. (*B*) Cumulative distribution of the interevent intervals calculated from the same experiment, in the indicated conditions. Treatment with the HCRTR-1 inhibitor prevented the stimulatory effect of hypocretin on IPSCs. The cumulative distributions of the interevent intervals in the presence SB 3 348 671 and in the presence of hypocretin + SB 3 348 671 were not significantly different (with KS test). (*C*) Similar results were obtained in 7 total experiments. Bars give the average steady-state IPSCs, in the indicated conditions, analyzed as in Figure 4. Hypocretin + SB 3 348 671 (SB) did not alter the average IPSC frequency, compared with both the control condition and treatment with the inhibitor alone. Detailed statistics are given in the main text.

usually reached the steady state within 1–2 min. The frequency of the mIPSCs did not change in the presence of 100 nM hypocretin 1. In a series of similar experiments (Fig. 6*B*), the average frequency of the miniature events (measured in 2 min intervals for the different conditions, at the steady state) was 1.24 ± 0.38 Hz in the presence of TTX and Cd^{2+} and 1.11 ± 0.32 Hz in the presence of TTX, Cd^{2+}, and hypocretin (NS; $n = 6$). Because Cd^{2+} blocks the voltage-gated Ca^{2+} channels, Figure 6*B* indicates that hypocretin 1 cannot produce sufficient release of Ca^{2+} from intracellular stores to significantly affect GABA release. We next repeated our experiments in the presence of TTX alone, to determine whether an increase in mIPSCs was produced by hypocretin when the voltage-gated Ca^{2+} channels were not inhibited. TTX produced a drastic decrease of IPSC frequency and amplitude (Fig. 6*C,D*), confirming that 0.5 μM TTX is sufficient to inhibit most of the action potential activity in our cells. In the absence of Cd^{2+}, hypocretin remained unable to increase the probability of GABA release. In particular, the average mIPSC frequency was 3.1 ± 0.36 in the presence of TTX, compared with 2.6 ± 0.3, in the presence of TTX plus 100 nM orexin (Fig. 6*C*; NS, $n = 5$). Similar results were obtained by increasing hypocretin concentration to 500 nM ($n = 7$; not shown). We conclude that tonic levels of hypocretin do not directly stimulate GABA release from interneuron terminals.

Hypocretin Effect on FS Cell Firing

Finally, we directly tested the effect of hypocretin 1 on FS-cell action potential firing. A series of experiments carried out in 2 mice litters is shown in Figure 7. FS interneurons were identified as shown in Figure 1. Before hypocretin application, V_{rest} was -71 ± 1.25 mV ($n = 5$). After testing cell firing, hypocretin (100 nM) was applied for 5 min. In agreement with the results shown in Figure 2, in the presence of hypocretin a 2- to 3-fold

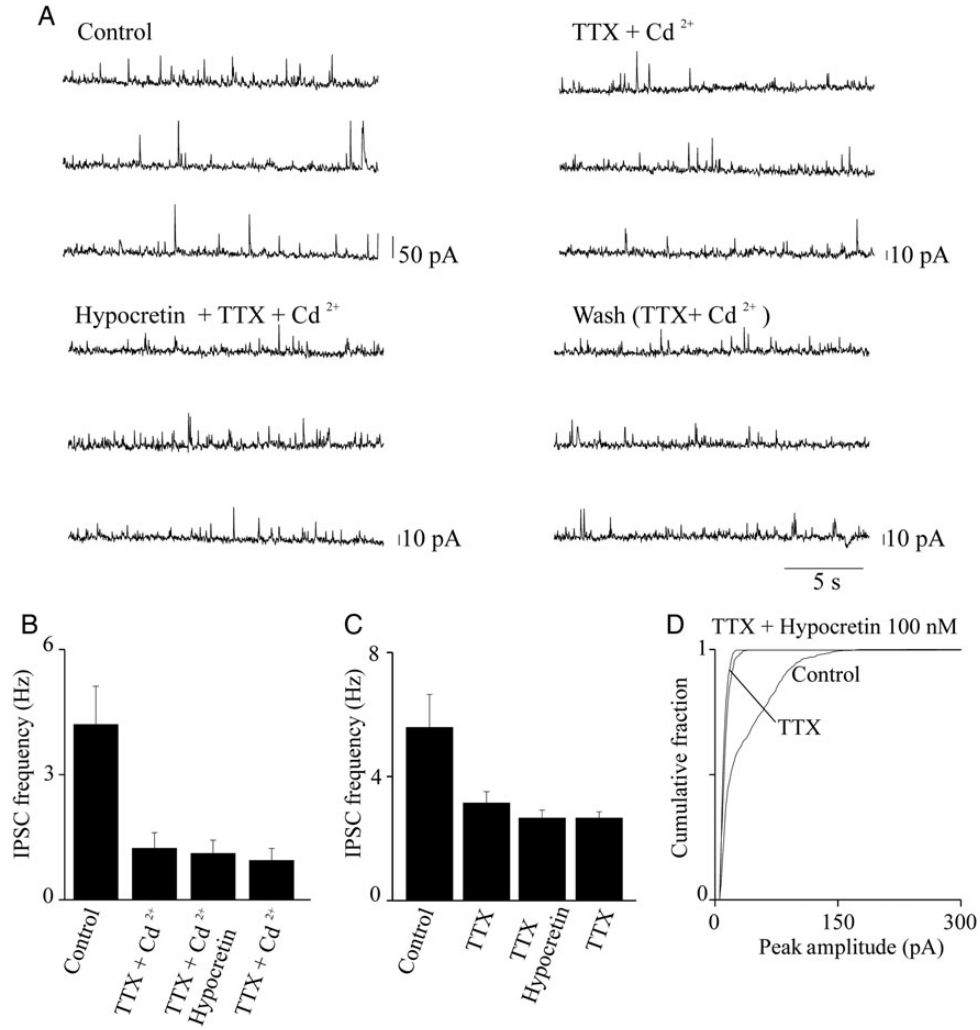

Figure 6. Hypocretin is ineffective on miniature IPSCs. (*A*) IPSC traces at +10 mV, from a representative pyramidal neuron. Traces illustrate ~60-s continuous recording before treatment (Control), in the presence of 0.5 μM TTX + 50 μM Cd^{2+} (TTX + Cd^{2+}), in the presence of 0.5 μM TTX, 50 μM Cd^{2+}, and 100 nM hypocretin 1 (Hypocretin + TTX + Cd^{2+}), and after removal of hypocretin (Wash). In this experiment, treatment with TTX + Cd^{2+} revealed the miniature IPSC events, whose frequency was considerably lower than the frequency of the spontaneous IPSCs. Hypocretin did not significantly alter the frequency of these miniature events (as estimated with KS test; not shown). (*B*) Similar results were obtained in 6 total experiments. Bars give the average effect of the indicated treatments on the IPSC frequency, calculated for 2-min continuous recording at the steady state, in each indicated condition ($n = 6$). Hypocretin did not produce any significant increase in the miniature IPSC frequency, as detailed in the main text. (*C*) Average results obtained from 5 experiments carried out and analyzed as illustrated in (*A*) and (*B*), except that Cd^{2+} was not present. Hypocretin did not produce any significant alteration in the average frequency of the miniature IPSCs (statistics are given in the main text). Similar results were obtained in the presence of 500 nM hypocretin ($n = 7$).

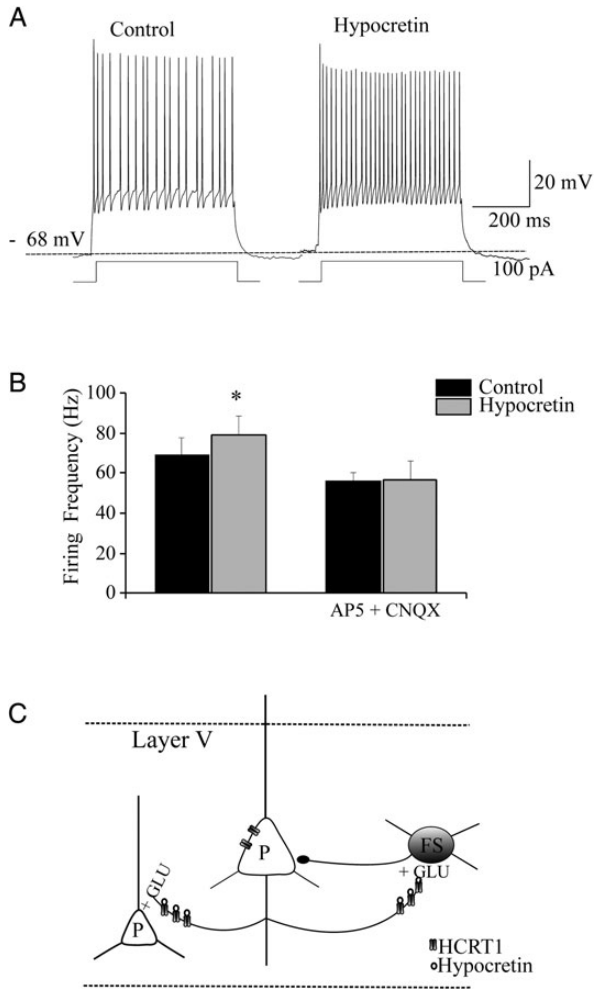

Figure 7. Hypocretin accelerates action potential firing in FS cells. (*A*) Cell firing in a representative FS cell, recorded as illustrated in Figure 1. Application of hypocretin 1 (100 nM) accelerated the firing rate. (*B*) Bars show the average results on FS firing produced by hypocretin in a series of experiments on cells in the same mice litters, in the absence (left bars) or in the presence (right bars) of 50 μM AP5 and 10 μM CNQX. Hypocretin brought the FS-cell firing frequency from 69.1 ± 8.46 to 79.03 ± 9.9 Hz (*$0.01 < P < 0.05$; $n = 5$). No effect was produced by the peptide in the presence of AP5 and CNQX, when the FS-cell firing frequency was 56.26 ± 4.08 Hz in the absence and 56.5 ± 9.52 Hz in the presence of hypocretin (NS; $n = 5$). The effects of hypocretin on V_{rest} were overall minor. In the absence of AP5 and CNQX, hypocretin brought V_{rest} from −71.1 ± 1.25 to −67.7 ± 1.83 mV (NS, $n = 5$); whereas in the presence of the blockers hypocretin brought V_{rest} from −65.2 ± 1.93 to −63 ± 2.85 mV (NS; $n = 5$). (*C*) Schematic of the Fr2 layer V network, with reference to the actions of hypocretin on pyramidal (P) and FS neurons.

increase in the frequency of the spontaneous EPSPs was generally observed. For example, in the representative cell whose firing is shown in Figure 7*A*, the frequency of EPSPs calculated during 60 s before the peptide was added was 1.4 Hz, while it increased to 3.02 Hz during 60 s in the presence of hypocretin. Figure 7*A* shows the elicited firing frequency in the absence and presence of the peptide. The average results of a series of such experiments are shown in Figure 7*B* (left bars), showing that hypocretin produced an ~15% increase of the FS-cell firing frequency. In contrast, no such effects were produced by the peptide in the presence of AP5 and CNQX (Fig. 7*B*; right bars). Detailed statistics are given in the figure legend. A schematic of the hypocretin transmission in Fr2 layer V is given in Figure 7*C*, which is based on both the patch-clamp experiments and the immunostaining results to be illustrated in the following paragraphs. The diagram is further discussed later.

HCRTR-1 Protein Expression in PFC and SS Cortex

The neocortical expression and distribution of HCRTR-1 was studied by immunodetection methods. HCRTR-1 was immunostained with an antibody developed against the sequence C-YNFLSGKFREQFK, located in the internal region of the protein. The antibody specificity was preliminarily assayed by immunoblot tests. As shown in Figure 8*A*, in fractions prepared from Fr2 and SS a protein band of ~50 kDa was detected, consistent with the expected molecular weight of the native HCRTR-1 (Guan et al. 2001). The densitometric analysis of immunoreactive bands, after normalization on the corresponding α-tubulin levels, shows that the expression of HCRTR-1 protein in Fr2 was about 20% higher than in SS cortex (Fig. 8*B*; statistics are given in the figure legend). Signal was absent in the controls (Fig. 8*A*). Next, we studied by immunocytochemistry the HCRTR-1 distribution in coronal sections of SS and Fr2. Confocal images were analyzed with constant acquisition parameters, to directly compare the fluorescence intensity in layer V of SS (Fig. 8*C*) and Fr2 (Fig. 8*D*). Higher magnification images are shown in Figure 8*C′* (SS), and Figure 8*D′* (Fr2). An intense and diffuse signal was observed, with immunoreactive spots on cell bodies of large and medium size neurons as well as in the neuropil. Overall, the signal was stronger in Fr2, compared with SS. In both regions, the neuronal and neuropilar stain was not homogeneously distributed in different layers. In Fr2, labeled cells tended to be concentrated in layer V, when compared with the supragranular layers. A weaker signal was observed in layer III, characterized by pyramidal cells of different sizes and nonpyramidal cells. A similar pattern was observed in SS (data not shown).

HCRTR-1 Distribution in GABAergic Elements

We next studied the neurochemical nature of the structures expressing HCRTR-1. Interneuron somata were distinguished by labeling parvalbumin (PV), which is expressed by FS neurons and chandelier cells (Rudy et al. 2011). The GABAergic fibers were identified by staining the GABA synthesizing enzyme glutamic acid decarboxylase GAD65. For comparison with the patch-clamp results, we show confocal images of layer V. Double staining with HCRTR-1/GAD65 showed little colocalization in both SS (not shown) and Fr2 (Fig. 9*A*). GAD65 mainly labeled inhibitory terminals that rarely expressed HCRTR-1. At higher magnification, scarce immunoreactive colocalization puncta were observed on terminals contacting the somata of HCRTR-1+ neurons (Fig. 9*A′*). Differently from GAD65, which labels all GABAergic cells, the anti-PV antibody localizes a subpopulation of interneurons, mostly constituted by FS cells (Rudy et al. 2011). Once again, virtually no colocalization was observed on PV+ terminals, while only a weak colocalization was observed on inhibitory interneuronal somata (Fig. 9*B*,*B′*). However, the colocalization of HCRTR-1 with both GAD65 and PV revealed a diffuse labeling on the cell bodies of a subpopulation of GABAergic interneurons expressing HCRTR-1 (Fig. 9*C*,*C′*,*C″*). Altogether, these results are consistent with the lack of effect of hypocretin 1 on the mIPSCs.

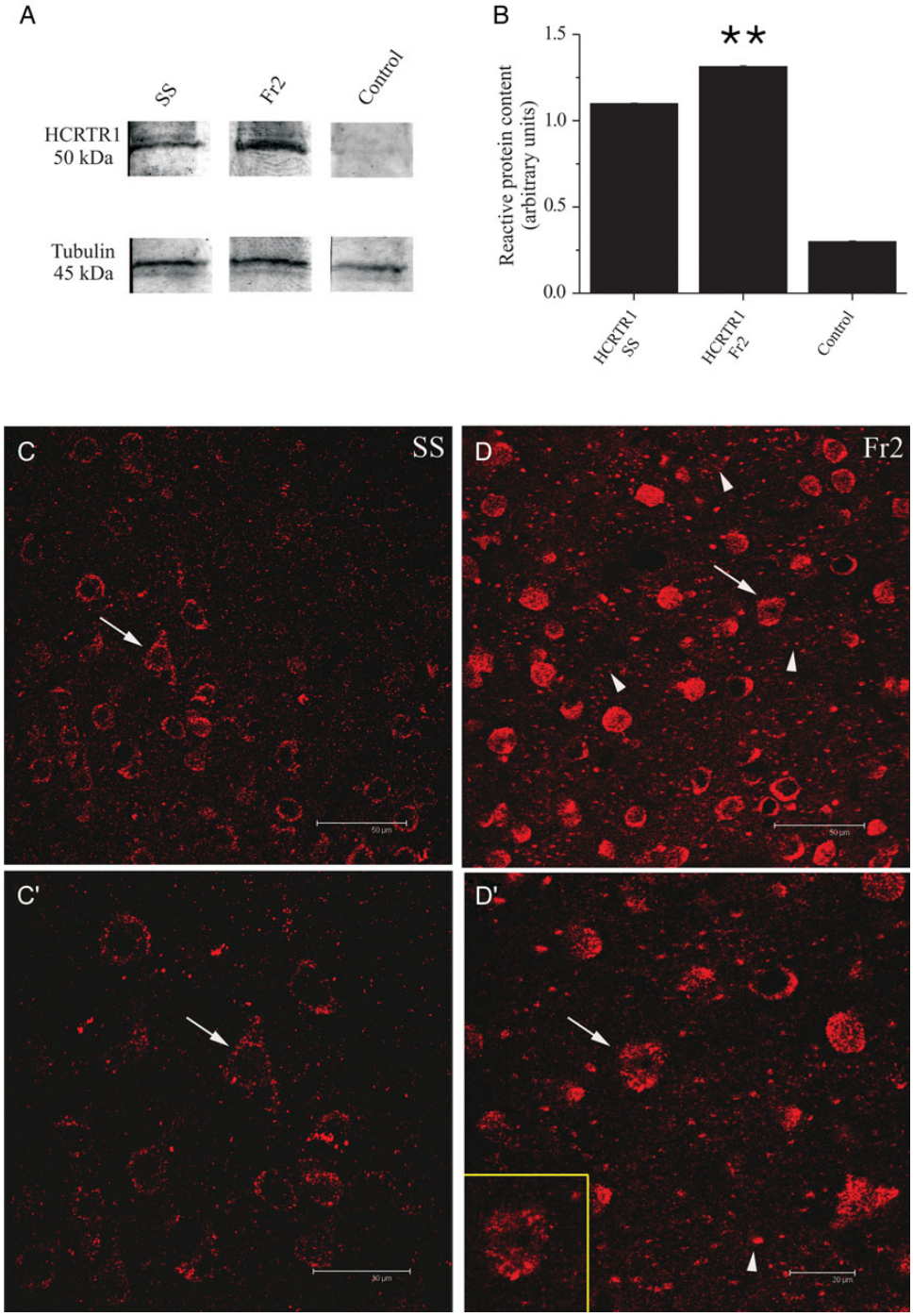

Figure 8. Western blot and immunocytochemical analysis of HCRTR-1 expression. (*A*) HCRTR-1 expression in membrane fractions of SS (lane 1) and Fr2 (lane 2). Data were obtained by using Mem-PER. The antibody against HCRTR-1 recognized a specific band with an apparent molecular mass of 50 kDa, consistent with the expression of the native HCRTR-1 (according to NP_001516.1 and Karteris et al. 2005). Equal protein loading was assayed by evaluating the total α-tubulin with a monoclonal anti-α-tubulin antibody as a loading control (lower panels; see Materials and Methods). Controls carried out using preadsorbed HCRTR-1 antiserum and with omission of primary HCRTR-1 antibody were completely negative (lane 3). (*B*) Comparison of the average intensity of the western blot bands calculated for 3 representative experiments, in the indicated conditions. Optical intensity was detected and analyzed as detailed in Materials and Methods. The immunoreactivity obtained with anti-HCRTR-1 was normalized to the one obtained with anti-α-tubulin, and the resulting ratios were plotted for both SS and Fr2, as indicated. In these tests, HCRTR-1 gave a mean value of 1.31 ± 0.006 for Fr2 and 1.10 ± 0.004 for SS (**$P < 0.01$; comparison between HCRTR-1 in SS and HCRTR-1 in Fr2). (*C*), (C′), (*D*), and (*D′*) illustrate the immunocytochemical analysis of HCRTR-1 expression. In layer V of SS (*C*), the HCRTR-1 granular immunoreactivity was mainly detected at the level of neuronal cell bodies sometimes clearly identifiable as pyramidal neurons, based on morphology (arrows). (*C′*) gives a higher magnification detail of (*C*). In layer V of Fr2 (*D*), the HCRTR-1 positive (+) signal was considerably more intense than in SS and was detectable not only in numerous cell bodies (arrows and inset in *D′*), but also in neuropilar processes of different caliber (arrowheads). (*D′*) gives a higher magnification detail of (*C*). Scale bars: 50 μm (*C*, *D*); 30 μm (*C′*); 20 μm (*D′*).

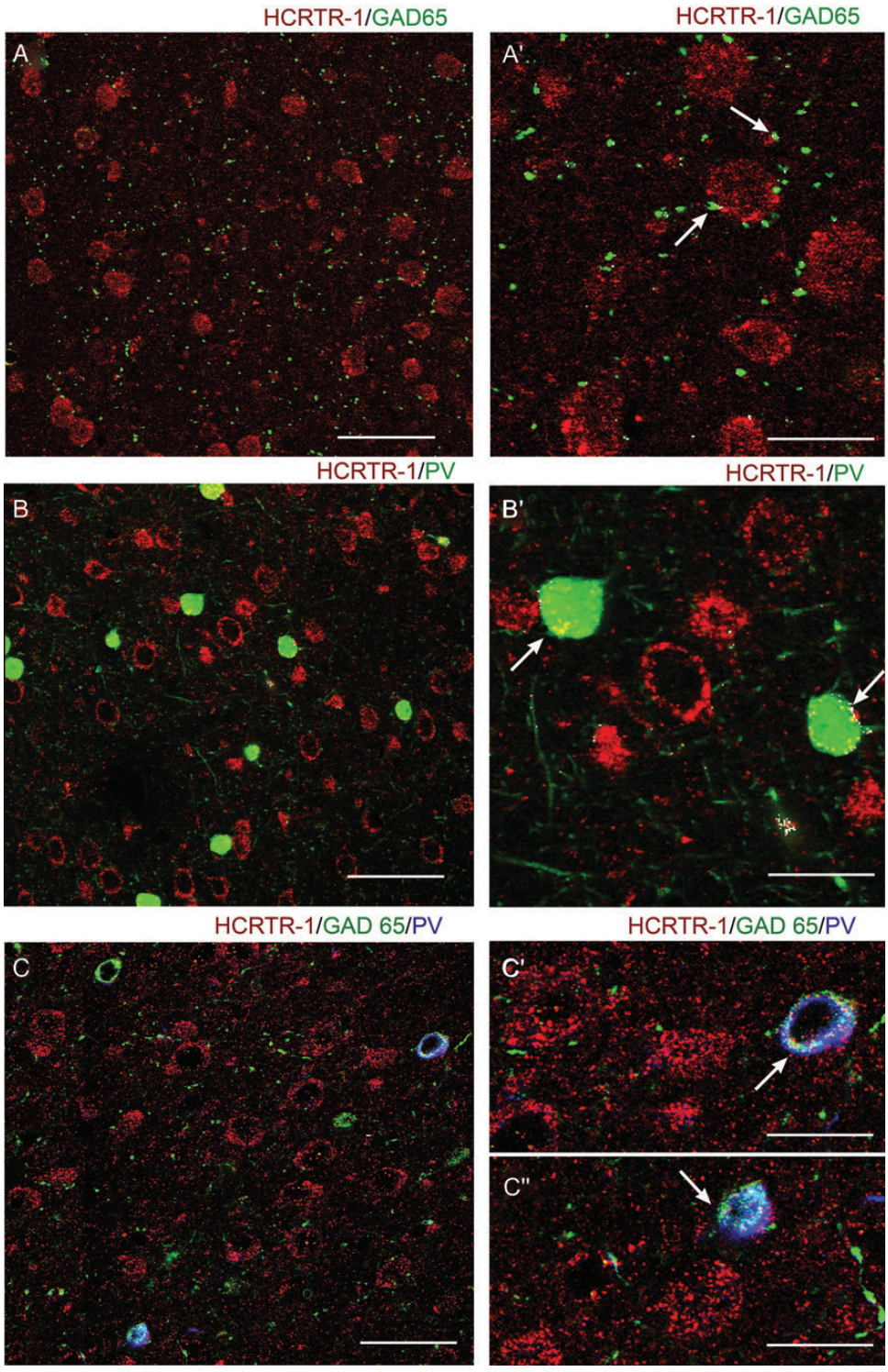

Figure 9. Expression of HCRTR-1 in GABAergic cells. Confocal microscopy images of double and triple immunofluorescent staining for HCRTR-1, glutamic acid decarboxylase (65 kDa form; GAD65), and/or parvalbumin (PV) in layer V of Fr2. (*A*) and (*A′*) show, at different magnification, the distribution of HCRTR-1 (red) and GAD65 (green). Very little colocalization (white signal) characterized hypocretin receptor and GABAergic inhibitory terminals (arrows) contacting HCRTR-1+ neurons or processes. (*B*) and (*B′*) show, at different magnification, the distribution of HCRTR-1 (red) and PV (green). Colocalization (white) was detected only in cell bodies of a few interneuronal inhibitory cells (arrows). (*C*), (*C′*), and (*C″*) show, at different magnification, immunolabeling of HCRTR-1 (red), GAD65 (green), and PV (blue). White signal marks triple colocalization. A subpopulation of PV + GABAergic (GAD65+) interneurons expressed HCRTR-1. Scale bars: 50 μm (*A*, *C*); 60 μm (*B*); 25 μm (*A′*); 20 μm (*B′*, *C′*, *C″*).

HCRTR-1 Distribution in Glutamatergic Elements

To better understand the role of HCRTR-1 in regulating glutamatergic transmission, we analyzed the receptor's colocalization with 2 well-known markers of glutamatergic terminals, the vesicular glutamate transporters VGLUT1 and VGLUT2. As was discussed earlier, by comparing the distribution of VGLUT1 and VGLUT2 one can assess the relative contribution of intracortical and extrinsic (mainly thalamocortical) glutamatergic fibers

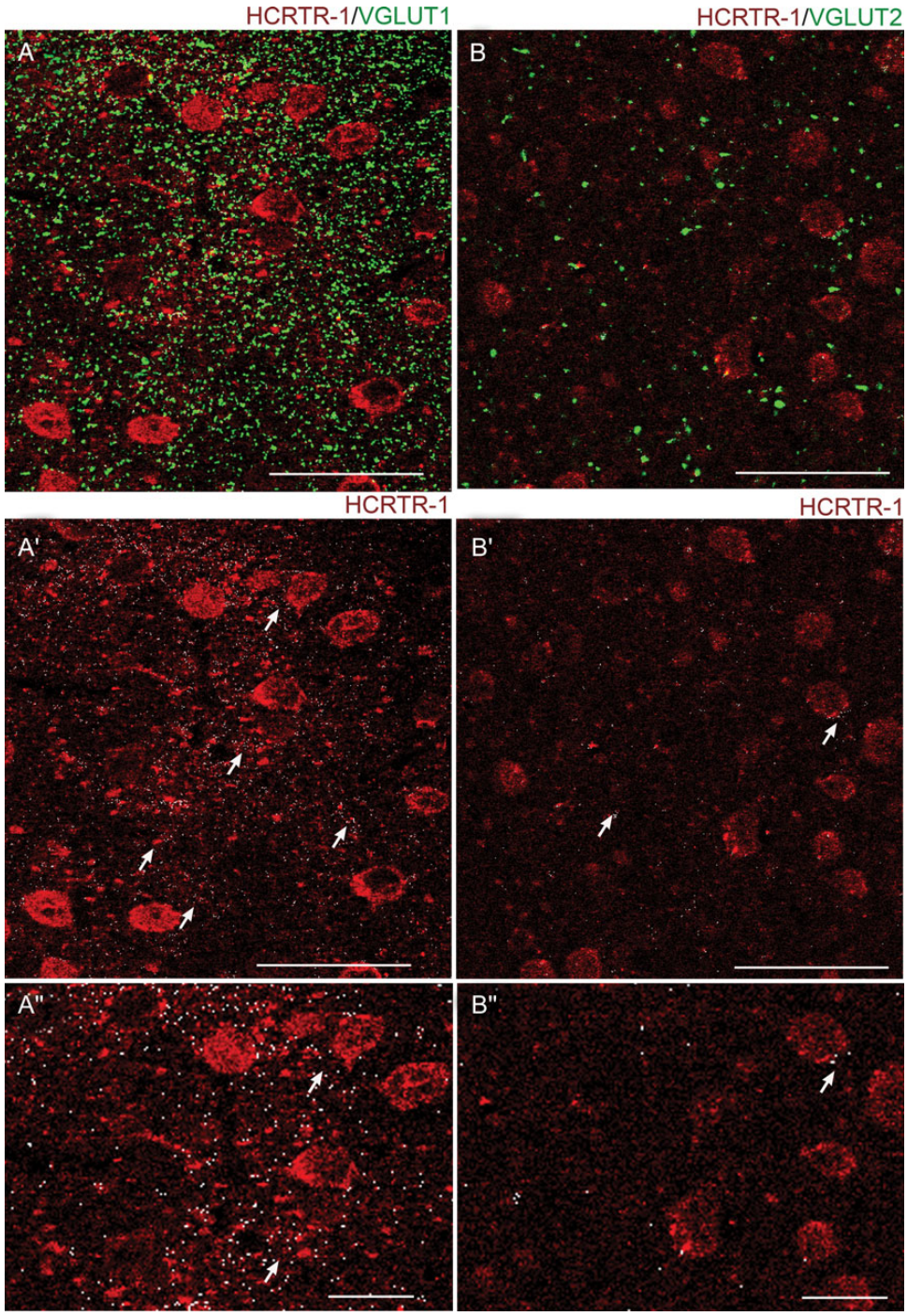

Figure 10. Expression of HCRTR-1 in VGLUT1+ and VGLUT2+ glutamatergic fibers in layer V of Fr2. (*A*) Confocal microscopy images of double immunofluorescent staining for HCRTR-1 (red) and VGLUT1 (green). White spots are colocalization puncta. For better distinction of the 2 signals, (*A′*) only shows the HCRTR-1 signal (red) plus the white colocalization puncta. (*A″*) is a higher magnification version of (*A′*). Overall, a high density of VGLUT1+ synaptic terminals was observed in the neuropil of Fr2 (*A*). Moreover, a high degree of colocalization was detected for our markers (see also the arrows in *A′*). (*B*) Confocal microscopy images of double immunofluorescent staining for HCRTR-1 (red) and VGLUT2 (green). White spots are colocalization puncta. For better distinction of the 2 signals, (*B′*) only shows the HCRTR-1 signal, plus the white colocalization puncta. (*B″*) is a higher magnification version of (*B′*). Only a few large VGLUT2+ synaptic terminals were present in layer V among the HCRTR-1+ elements. The colocalization (white) was scarce as also indicated by the arrows in (*B′*). Scale bars: 50 μm for (*A*), (*A′*), (*B*), (*B′*); 20 μm for (*A″*) and (*B″*).

(Hur and Zaborsky 2005; Nakamura et al. 2005; Graziano et al. 2008). Double labeling for HCRTR-1 and VGLUT1 revealed widespread colocalization on the neuropilar synaptic terminals that take contact with the HCRTR-1+ neuronal cell bodies (Fig. 10*A*,*A′*,*A″*). Once again, a similar pattern was observed in SS, although the signal for HCRTR-1 tended to be generally weaker (data not shown). Instead, double labeling for HCRTR-1 and VGLUT2 revealed scarce colocalization in both SS (not shown) and Fr2 (Fig. 10*B*,*B′*,*B″*), indicating that HCRTR-1 is scarcely expressed in the extrinsic afferent fibers, in Fr2.

Discussion

The mechanism by which hypothalamic hypocretin neurons regulate the neocortical tone is extremely complex. Neuroanatomical and microdialysis studies indicate that hypocretin cells stimulate the ascending regulatory pathways, thus leading to intracortical release of norepinephrine (Horvath et al. 1999), histamine (Huang et al. 2001), acetylcholine (Fadel et al. 2005; del Cid-Pellitero and Garzón 2011), and dopamine (Vittoz and Berridge 2006). Moreover, hypocretin fibers innervate the thalamus (Peyron et al. 1998) and direct stimulation of the midline-intralaminar glutamatergic thalamocortical cells has been observed (Bayer et al. 2002). It should be also mentioned that hypocretin neurons have been also shown to release glutamate in histaminergic neurons (Schöne et al. 2012), and possibly in the locus coeruleus (Henny et al. 2010). The hypocretin system is thought to integrate the metabolic and behavioral information to generate the level of arousal appropriate for the different behavioral tasks during wakefulness. A major physiological stimulus on hypocretin cells is the overall metabolic state of the organism (Yamanaka et al. 2003) and particularly the balance of macronutrients (Karnani et al. 2011). However, increasing evidence points to specific actions of the hypocretin signals in the prefrontal executive functions and intrinsic hypocretin-dependent signaling mechanisms have been identified in the PFC.

Hypocretin Fibers and Receptors in the PFC

Extensive evidence is available in the rat, whose neocortex shows widespread hypocretin fibers (Peyron et al. 1998), as well as clear expression of HCRTR-1 and HCRTR-2 (Hervieu et al. 2001; Marcus et al. 2001). In general, a sparse to moderate innervation of the frontal regions is observed (Cutler et al. 1999; Date et al. 1999; Nambu et al. 1999; Baldo et al. 2003). The density of hypocretin axons is higher in the infra- and prelimbic cortex (Baldo et al. 2003) and lower in dorsal regions (Fadel and Deutch 2002). The laminar distribution of hypocretin fibers tends to be denser in layers I, II, V, VI, and especially in the subgranular layers, and sparser in layers III and IV. This reinforces the notion that hypocretin is particularly related to the PFC output to subcortical regions and thus to the executive functions. In fact, the apical dendrite tufts of layer V pyramidal neurons in the medial PFC are sensitive to hypocretin (Liu and Aghajanian 2008). Our observation that HCRTR-1 is conspicuously expressed in Fr2 layer V agrees with the evidence in rats. Although detailed morphological comparisons of the hypocretin system between different PFC regions and layers are not available, heavy HCRTR-1 protein labeling is present in the primary and secondary motor areas in the rat (Hervieu et al. 2001), and HCRTR-1 mRNA is generally detected in layer V (Marcus et al. 2001). Because HCRTR-1 strongly colocalized with VGLUT1, but not VGLUT2, we conclude that the receptor's expression tends to be concentrated on intracortical glutamatergic fibers when compared with the extrinsic excitatory fibers (mostly thalamocortical). The expression of HCRTR-1 in glutamatergic terminals is consistent with the effect of the peptide on the mEPSCs (Fig. 3). The overall block produced by SB-334867 on the hypocretin-dependent synaptic effects confirms the prominent role of HCRTR-1 in Fr2. Our results are in reasonable agreement with the only other comparable study available in the mouse, as Li et al. (2010) recently observed a dense expression of HCRTR-1 in layer V of the prelimbic PFC, which prevailed on that of HCRTR-2 on both somata and dendrites of pyramidal cells.

The Role of Hypocretin in the Prefrontal Network

Until now, the physiological studies have mainly focused on the medial PFC. However, morphological and functional heterogeneity is increasingly recognized to characterize the PFC (Franklin and Chudasama 2011). In the mouse, detailed comparisons between the different prefrontal areas are scarce (Van de Werd et al. 2010; Franklin and Chudasama 2011; Paulussen et al. 2011). This increases the interpretative difficulties, especially if one intends to extrapolate the conclusions drawn from murine models to the pathophysiology of the highly complex dorsolateral PFC of primates (Uylings et al. 2003). We focused on the prefrontal Fr2 region, which we hypothesize to be particularly relevant for the attentive effects of hypocretins. In fact, Fr2 is implicated in the behavioral response to environmental contexts that require quick attention and has probably an important role in mediating the motivation-dependent goal-oriented tasks (Hoover and Vertes 2007; Kargo et al. 2007). Fr2 displays peculiar cytoarchitectonic features. In general, the supragranular layer thickness tends to decrease from the lateral to the medial PFC (Kirkcaldie et al. 2002; Van de Werd et al. 2010; Franklin and Chudasama 2011; Aracri et al. 2013). More specifically, the balance of pyramidal cells and interneurons seems different among PFC regions (Helmeke et al. 2008; Aracri et al. 2013), and basket cells display a more homogeneous laminar distribution in Fr2 (Aracri et al. 2013).

In rodents, direct evidence that hypocretin exerts behavioral roles in the neocortex was first shown by infusing the peptide into the PFC, which increases the attentive tasks in rats (Lambe et al. 2005). In addition, recent evidence in hypocretin knockout mice shows that the medial PFC is a major mediator of the mechanism leading from positive emotions to cataplexy (Oishi et al. 2013). In parallel, electrophysiological studies have begun to unravel the detailed hypocretin actions in the neocortex. Both pre- and postsynaptic effects have been observed in the infragranular layers, in agreement with the discussed pattern of HCRTR expression. In the rat primary SS cortex, hypocretin was found to stimulate pyramidal neurons in sublayer 6b. The effect is postsynaptic, it is mediated by HCRTR2 and is not observed in layers II–V. The sublayer specificity was also observed in the primary visual cortex, the primary motor cortex, and the cingulate cortex (Bayer et al. 2004). Neurons in sublayer 6b send extensive corticocortical projections, especially to layer I (Clancy and Cauller 1999), with ensuing activations of neurons located in deeper layers. This local activating mechanism supplements the hypocretin-dependent modulation of the nonspecific thalamocortical nuclei (Bayer et al. 2002). Therefore, in primary cortices, hypocretin seems to produce a widespread cortical activation by coupling the stimulation of thalamocortical afferents with direct regulation of pyramidal neurons.

In the associative cortices, the pattern appears to be more complex. In rat anterior cingulate cortex, hypocretin is able to stimulate layer V pyramidal neurons by HCRTR-2-mediated stimulation of glutamate release from thalamocortical terminals, thus cooperating with the effect of acetylcholine on the same terminals (Lambe and Aghajanian 2003; Lambe et al. 2005). This mechanism appears to be absent in the parietal cortex (Lambe and Aghajanian 2003). In the murine prelimbic cortex, HCRTR-1 was found to be expressed in layer V

pyramidal neurons, thus permitting a postsynaptic action of hypocretin mediated by regulation of HCN currents (Li et al. 2010). Although we did not test this mechanism in Fr2, part of the hypocretin-dependent glutamatergic stimulation we observed may depend on a similar effect, in addition to the presynaptic modulation. Although the evidence is still fragmentary, it appears that specific hypocretin-dependent mechanisms are found in different prefrontal regions with different physiological functions, which certainly merits further investigation.

From a comparative point of view, the results obtained in mice are broadly in line with the studies related to narcolepsy in nonrodent mammalian species. In fact, HCRTR-1 expression markedly decreases in humans affected by narcolepsy/cataplexy as well as in dogs exhibiting sporadic narcolepsy (Mishima et al. 2008). Conversely, HCRTR-1 deletion generally produces milder effects on the sleep-waking cycle, compared with the deletion of HCRTR-2 (Sakurai 2007). Therefore, the preferential expression of HCRTR-1 we observed in corticocortical fibers, when compared with the thalamocortical, supports the notion that HCRTR-1 is especially implicated in sustaining arousal and regulating synaptic transmission in the PFC during wakefulness, and less so in controlling the transition between different brain states.

Hypocretin and GABAergic Cells in Fr2 Layer V

To better determine the role of hypocretin in the neocortical circuits, we studied the effect of hypocretin 1 on FS cells. Our results can be summarized as follows. First, hypocretin produced a moderate but reproducible increase of GABA release (sIPSCs) onto regular spiking pyramidal cells. The effect of the peptide on GABAergic transmission is confirmed by the stimulation produced by the peptide on FS-cell firing. However, immunocytochemistry shows little colocalization of HCRTR-1 with GAD65 and PV, which is consistent with the scarce effect produced by hypocretin on both FS-cells' V_{rest} and miniature GABAergic currents. This indicates there is little direct effect of the peptide on most basket cells. Because hypocretin stimulated glutamate release onto FS cells, a likely explanation of our findings is that the peptide contributes to regulate layer V inhibitory cells indirectly, by regulating the glutamatergic drive onto FS cells (a scheme is given in Fig. 7*C*). This hypothesis agrees with the observation that the hypocretin-dependent stimulations of FS-cell firing and of GABA release onto pyramidal cells were both abolished when the ionotropic glutamate receptors were blocked. Nonetheless, the data illustrated in Figure 9 indicate that a subpopulation of PV+/GAD65+ cells does present a detectable expression of HCRTR-1. Therefore, further studies are necessary to fully clarify the neurochemical nature of the subpopulations of HCRTR-1 expressing GABAergic cells, to be able to discriminate by electrophysiological methods their contribution to the local neocortical circuits. At the present stage, we interpret our results as indicating that in most basket cells the direct effects of tonic levels of hypocretin are weak.

No other reports about hypocretin regulation of neocortical interneurons are available in any species, to the best of our knowledge. The available studies of the action of hypocretin on murine hypothalamus show both direct and indirect regulation of inhibitory cells. In the arcuate nucleus, which controls feeding and energy homeostasis, GABAergic cells were found to be directly excited by an HCRTR-2-dependent stimulus of the Na^+/Ca^{2+} exchanger (Burdakov et al. 2003). On the other hand, a recurrent feedback inhibition has been recently demonstrated between hypocretin excitatory neurons and local interneurons (which express HCRTR-1; Matsuki et al. 2009). Our results in Fr2 show somewhat more resemblance with the latter mechanism, although, in our case, hypocretin seems to regulate the classical recurrent inhibition on pyramidal neurons.

Conclusions

A further conclusion suggested by our results is that hypocretin has a relatively potent steady-state effect on neurotransmitter release, in Fr2. This indicates that the peptide could produce appreciable physiological effects on the neocortical network in relative independence of the input provided by the classical regulatory neurotransmitter systems. Regardless, the interplay between hypocretin and the fibers of the ascending regulatory systems remains to be determined. Current evidence in medial PFC indicates that such interplay occurs at least with the acetylcholine nicotinic receptors expressed in the thalamocortical fibers (Lambe and Aghajanian 2003) and with the serotonergic inputs onto pyramidal cells (Liu and Aghajanian 2008). Moreover, because nicotinic receptors are widely expressed by the intrinsic glutamatergic fibers in Fr2 (Aracri et al. 2013), our present results suggest that hypocretin may cooperate with the cholinergic modulation of glutamate release, thus adding a further degree of flexibility to the intracortical glutamatergic transmission. Finally, the possibility we suggest that hypocretin may also regulate FS-cells' feedback onto pyramidal neurons encourages more detailed studies on the role of this peptide in the PFC local circuits, to determine the balance between generalized arousal effects and more specific local roles in synaptic transmission.

Funding

This work was supported by the Fondazione Banca del Monte di Lombardia; the University of Milano-Bicocca (FAR), and the Italian Telethon Foundation (grant number GGP12147). Funding to pay the Open Access publication charges for this article was provided by Telethon Italia.

Notes

Part of this work was carried out in CIMA, an advanced microscopy laboratory established by the University of Milan. *Conflict of Interest*: None declared.

References

Adamantidis AR, Zhang F, Aravanis AM, Deisseroth K, de Lecea L. 2007. Neural substrates of awakening probed with optogenetic control of hypocretin neurons. Nature. 450:420–424.

Ammoun S, Holmqvist T, Shariatmadari R, Oonk HB, Detheux M, Parmentier M, Akerman KE, Kukkonen JP. 2003. Distinct recognition of OX1 and OX2 receptors by orexin peptides. J Pharmacol Exp Ther. 305:507–514.

Aracri P, Amadeo A, Pasini ME, Fascio U, Becchetti A. 2013. Regulation of glutamate release by heteromeric nicotinic receptors in layer V of the secondary motor region (Fr2) in the dorsomedial shoulder of prefrontal cortex in mouse. Synapse. 67:338–357.

Aracri P, Consonni S, Morini R, Perrella M, Rodighiero S, Amadeo A, Becchetti A. 2010. Tonic modulation of GABA release by nicotinic acetylcholine receptors, in layer V of the murine prefrontal cortex. Cereb Cortex. 20:1539–1555.

Bacci A, Rudolph U, Huguenard JR, Prince DA. 2003. Major differences in inhibitory synaptic transmission onto two neocortical interneuron subclasses. J Neurosci. 23:9664–9674.
Baldo BA, Daniel RA, Berridge CW, Kelley AE. 2003. Overlapping distributions of orexin/hypocretin- and dopamine-β-hydroxylase immunoreactive fibers in rat brain regions mediating arousal, motivation, and stress. J Comp Neurol. 464:220–237.
Bayer L, Eggermann E, Saint-Mleux B, Machard D, Jones BE, Mühlethaler M, Serafin M. 2002. Selective action of orexin (hypocretin) on nonspecific thalamocortical projection neurons. J Neurosci. 22:7835–7839.
Bayer L, Eggermann E, Serafin M, Saint-Mleux B, Machard D, Jones B, Mühlethaler M. 2001. Orexins (hypocretins) directly excite tuberomammillary neurons. Eur J Neurosci. 14:1571–1575.
Bayer L, Serafin M, Eggermann E, Saint-Mleux B, Machard D, Jones BE, Mühlethaler M. 2004. Exclusive postsynaptic action of hypocretin-orexin on sublayer 6b cortical neurons. J Neurosci. 24:6760–6764.
Berendsee HW, Galis-de Graaf Y, Groenewegen HJ. 1992. Topographical organization and relationship with ventral striatal compartments of prefrontal corticostriatal projections in the rat. J Comp Neurol. 316:314–347.
Beuckmann CT, Yanagisawa M. 2002. Orexins: from neuropeptides to energy homeostasis and sleep/wake regulation. J Mol Med. 80:329–342.
Boutrel B, Cannella N, de Lecea L. 2010. The role of hypocretin in driving arousal and goal-oriented behaviors. Brain Res. 1314:103–111.
Burdakov D, Liss B, Ashcroft FM. 2003. Orexin excites GABAergic neurons of the arcuate nucleus by activating the sodium-calcium exchanger. J Neurosci. 23:4951–4957.
Chemelli RM, Willie JT, Sinton CM, Elmquist JK, Scammell T, Lee C, Richardson JA, Williams SC, Xiong Y, Kisanuki Y et al. 1999. Narcolepsy in orexin knockout mice: molecular genetics of sleep regulation. Cell. 98:437–451.
Clancy B, Cauller LJ. 1999. Widespread projections from subgriseal neurons (layer VII) to layer I in adult rat cortex. J Comp Neurol. 407:275–286.
Condé F, Maire-Lepoivre E, Audinat E, Crépel F. 1995. Afferent connections of the medial frontal cortex of the rat. II. Cortical and subcortical afferents. J Comp Neurol. 352:567–593.
Connors BW, Gutnick MJ. 1990. Intrinsic firing patterns of diverse neocortical neurons. Trends Neurosci. 13:99–104.
Couey JJ, Meredith RM, Spijker S, Poorthuis RB, Smit AB, Brussaard AB, Mansvelder HD. 2007. Distributed network actions by nicotine increase the threshold for spike-timing-dependent plasticity in prefrontal cortex. Neuron. 54:73–87.
Cutler DJ, Morris R, Sheridhar V, Wattam TA, Holmes S, Patel S, Arch JR, Wilson S, Buckingham RE, Evans ML et al. 1999. Differential distribution of orexin-A and orexin-B immunoreactivity in the rat brain and spinal cord. Peptides. 20:1455–1470.
Date Y, Ueta Y, Yamashita H, Yamaguchi H, Matsukura S, Kangawa K, Sakurai T, Yanagisawa M, Nakazato M. 1999. Orexins, orexigenic hypothalamic peptides, interact with autonomic, neuroendocrine and neuroregulatory systems. Proc Natl Acad Sci USA. 96:748–753.
del Cid-Pellitero E, Garzón M. 2011. Hypocretin1/OrexinA axon targeting of laterodorsal tegmental nucleus neurons projecting to the rat medial prefrontal cortex. Cereb Cortex. 21:2762–2773.
De Lecea L, Kilduff TS, Peyron C, Gao X, Foye PE, Danielson PE, Fukuhara C, Battenberg EL, Gautvik VT, Bartlett FS 2nd et al. 1998. The hypocretins: hypothalamus-specific peptides with neuroexcitatory activity. Proc Natl Acad Sci USA. 95:322–327.
Douglas RJ, Martin KAC. 2004. Neuronal circuits of the neocortex. Annu Rev Neurosci. 27:419–451.
Eggermann E, Serafin M, Bayer L, Machard D, Saint-Mleux B, Jones BE, Mühlethaler M. 2001. Orexins/hypocretins excite basal forebrain cholinergic neurones. Neuroscience. 108:177–181.
Eriksson KS, Sergeeva O, Brown RE, Haas HL. 2001. Orexin/hypocretin excites the histaminergic neurons of the tuberomammillary nucleus. J Neurosci. 21:9273–9279.
Fadel J, Deutch AY. 2002. Anatomical substrates of orexin-dopamine interactions: lateral hypothalamic projections to the ventral tegmental area. Neuroscience. 111:379–387.
Fadel J, Pasumarthi R, Reznikov LR. 2005. Stimulation of cortical acetylcholine release by orexin A. Neuroscience. 130:541–547.
Franklin KJB, Chudasama Y. 2011. The prefrontal cortex. In: Watson C, Paxinos G, Puelles L, editors. The mouse nervous system. Amsterdam (The Netherlands): Elsevier Academic Press. pp. 727–735.
Gerashchenko D, Blanco-Centurion C, Greco MA, Shiromani PJ. 2003. Effects of lateral hypothalamic lesion with the neurotoxin hypocretin-2-saporin on sleep in Long-Evans rats. Neuroscience. 116:223–235.
Gonchar Y, Wang Q, Burkhalter A. 2008. Multiple distinct subtypes of GABAergic neurons in mouse visual cortex identified by triple immunostaining. Front Neuroanat. 1:3.
Graziano A, Liu XB, Murray KD, Jones EG. 2008. Vesicular glutamate transporters define two sets of glutamatergic afferents to the somatosensory thalamus and two thalamocortical projections in the mouse. J Comp Neurol. 507:1258–1276.
Guan JL, Saotome T, Wang QP, Funahashi H, Hori T, Tanaka S, Shioda S. 2001. Orexinergic innervation of POMC-containing neurons in the rat arcuate nucleus. Neuroreport. 12:547–551.
Hagan JJ, Leslie RA, Patel S, Evans ML, Wattam TA, Holmes S, Benham CD, Taylor SG, Routledge C, Hemmati P et al. 1999. Orexin A activates locus coeruleus cell firing and increases arousal in the rat. Proc Natl Acad Sci USA. 96:10911–10916.
Heidbreder CA, Groenewegen HJ. 2003. The medial prefrontal cortex in the rat: evidence for a dorso-ventral distinction based upon functional and anatomical characteristics. Neurosci Biobehav Rev. 27:555–579.
Helmeke C, Ovtscharoff W Jr, Poeggel G, Braun K. 2008. Imbalance of immunohistochemically characterized interneuron populations in the adolescent and adult rodent medial prefrontal cortex after repeated exposure to neonatal separation stress. Neuroscience. 152:18–28.
Henny P, Brischoux F, Mainville L, Stroh T, Jones BE. 2010. Immunohistochemical evidence for synaptic release of glutamate from orexin terminals in the locus coeruleus. Neuroscience. 169:1150–1157.
Hervieu GJ, Cluderay JE, Harrison DC, Roberts JC, Leslie RA. 2001. Gene expression and protein distribution of the orexin-1 receptor in the rat brain and spinal cord. Neuroscience. 103:777–797.
Holmqvist T, Akerman KE, Kukkonen JP. 2001. High specificity of human orexin receptors for orexins over neuropeptide Y and other neuropeptides. Neurosci Lett. 305:177–180.
Hoover WB, Vertes RP. 2007. Anatomical analysis of afferent projections to the medial prefrontal cortex in the rat. Brain Struct Funct. 212:149–179.
Horvath TL, Peyron C, Diano S, Ivanov A, Aston-Jones G, Kilduff TS, van den Pol AN. 1999. Hypocretin (orexin) activation and synaptic innervation of the locus coeruleus noradrenergic system. J Comp Neurol. 415:145–159.
Huang ZL, Qu WM, Li WD, Mochizuki T, Eguchi N, Watanabe T, Urade Y, Hayaishi O. 2001. Arousal effect of orexin A depends on activation of the histaminergic system. Proc Natl Acad Sci USA. 98:9965–9970.
Hur EE, Zaborsky L. 2005. Vglut2 afferents to the medial prefrontal and primary somatosensory cortices: a combined retrograde tracing in situ hybridization study. J Comp Neurol. 483:351–373.
Jones BE. 2008. Modulation of cortical activation and behavioral arousal by cholinergic and orexinergic systems. Ann NY Acad Sci. 1129:26–34.
Kane JK, Tanaka H, Parker SL, Yanagisawa M, Li MD. 2000. Sensitivity of orexin-A binding to phospholipase C inhibitors, neuropeptide Y and secretin. Biochem Biophys Res Commun. 272:959–965.
Kargo WJ, Szatmary B, Nitz DA. 2007. Adaptation of prefrontal cortical firing patterns and their fidelity to changes in action-reward contingencies. J Neurosci. 27:3548–3559.
Karnani MM, Apergis-Schoute J, Adamantidis A, Jensen LT, de Lecea L, Fugger L, Burdakov D. 2011. Activation of central orexin/hypocretin neurons by dietary amino acids. Neuron. 72:616–629.

Karteris E, Machado RJ, Chen J, Zervou S, Hillhouse EW, Randeva HS. 2005. Food deprivation differentially modulates orexin receptor expression and signaling in rat hypothalamus and adrenal cortex. Am J Physiol Endocrinol Metab. 288:E1089–E1100.
Kawaguchi Y, Kondo S. 2002. Parvalbumin, somatostatin and cholecystokinin as chemical markers for specific GABAergic interneuron types in the rat frontal cortex. J Neurocytol. 31:277–287.
Kawaguchi Y, Kubota Y. 1997. GABAergic cell subtypes and their synaptic connections in rat frontal cortex. Cereb Cortex. 7:476–486.
Kiritoshi T, Sun H, Ren W, Stauffer SR, Lindsley CW, Conn PJ, Neugebauer V. 2013. Modulation of pyramidal cell output in the medial prefrontal cortex by mGluR5 interacting with CB1. Neuropharmacology. 66:170–178.
Kirkcaldie MT, Dickson TC, King CE, Grasby D, Riederer BM, Vickens JC. 2002. Neurofilament triplet proteins are restricted to a subset of neurons in the rat neocortex. J Chem Neuroanat. 24:163–171.
Kohlmeier KA, Watanabe S, Tyler CJ, Burlet S, Leonard CS. 2008. Dual orexin actions on dorsal raphe and laterodorsal tegmentum neurons: noisy cation current activation and selective enhancement of Ca2+ transients mediated by L-type calcium channels. J Neurophysiol. 100:2265–2281.
Kubota Y, Shigematsu N, Karube F, Sekigawa A, Kato S, Yamaguchi N, Hirai Y, Morishima M, Kawaguchi Y. 2011. Selective coexpression of multiple chemical markers defines discrete populations of neocortical GABAergic neurons. Cereb Cortex. 21:1803–1817.
Kukkonen JP. 2013. Physiology of the orexinergic/hypocretinergic system: a revisit in 2012. Am J Physiol Cell Physiol. 304:C2–C32.
Lambe EK, Aghajanian GK. 2003. Hypocretin (orexin) induces calcium transients in single spines postsynaptic to identified thalamocortical boutons in prefrontal slice. Neuron. 40:139–150.
Lambe EK, Liu R-J, Aghajanian GK. 2007. Schizophrenia, hypocretin (orexin), and the thalamocortical activating system. Schizophrenia Bull. 33:1284–1290.
Lambe EK, Olausson P, Horst NK, Taylor JR, Aghajanian GK. 2005. Hypocretin and nicotine excite the same thalamocortical synapses in prefrontal cortex: correlation with improved attention in rat. J Neurosci. 25:5225–5229.
Lee MG, Hassani OK, Jones BE. 2005. Discharge of identified orexin/hypocretin neurons across the sleep-waking cycle. J Neurosci. 25:6716–6720.
Li B, Chen F, Ye J, Chen X, Yan J, Li Y, Xiong Y, Zhou Z, Xia J, Hu Z. 2010. The modulation of orexin A on HCN currents of pyramidal neurons in mouse prelimbic cortex. Cereb Cortex. 20:1756–1767.
Lin L, Faraco J, Li R, Kadotani H, Rogers W, Lin X, Qiu X, de Jong PJ, Nishino S, Mignot E. 1999. The sleep disorder canine narcolepsy is caused by a mutation in the hypocretin (orexin) receptor 2 gene. Cell. 98:365–376.
Liu RJ, Aghajanian GK. 2008. Stress blunts serotonin- and hypocretin-evoked EPSCs in prefrontal cortex: role of corticosterone-mediated apical dendrite atrophy. Proc Natl Acad Sci USA. 105:359–364.
Liu RJ, van den Pol AN, Aghajanian GK. 2002. Hypocretins (orexins) regulate serotonin neurons in the dorsal raphe nucleus by excitatory direct and inhibitory indirect actions. J Neurosci. 22:9453–9464.
Marcus JN, Aschkenasi CJ, Lee CE, Chemelli RM, Saper CB, Yanagisawa M, Elmquist JK. 2001. Differential expression of orexin receptors 1 and 2 in the rat brain. J Comp Neurol. 435:6–25.
Matsuki T, Nomiyama M, Takahira H, Hirashima N, Kunita S, Takahashi S, Yagami K, Kilduff TS, Bettler B, Yanagisawa M et al. 2009. Selective loss of $GABA_B$ receptors in orexin-producing neurons results in disrupted sleep/wakefulness architecture. Proc Natl Acad Sci USA. 106:4459–4464.
Mileykovskiy BY, Kiyashchenko LI, Siegel JM. 2005. Behavioral correlates of activity in identified orexin/hypocretin neurons. Neuron. 46:787–798.
Mishima K, Fujiki N, Yoshida Y, Sakurai T, Honda M, Mignot E, Nishino S. 2008. Hypocretin receptor expression in canine and murine narcolepsy models and in hypocretin-ligand deficient human narcolepsy. Sleep. 31:1119–1126.
Nakamura K, Hioki H, Fujiyama F, Kaneko T. 2005. Postnatal changes of vesicular glutamate transporter (VGluT)1 and VGluT2 immunoreactivities and their colocalization in the mouse forebrain. J Comp Neurol. 492:263–288.
Nambu T, Sakurai T, Mizukami K, Hosoya Y, Yanagisawa M, Goto K. 1999. Distribution of orexin neurons in the adult rat brain. Brain Res. 827:243–260.
Ohno K, Sakurai T. 2008. Orexin neuronal circuitry: role in the regulation of sleep and wakefulness. Front Neuroendocrinol. 29:70–87.
Oishi Y, Williams RH, Agostinelli L, Arrigoni E, Fuller PM, Mochizuki T, Saper CB, Scammell TE. 2013. Role of the medial prefrontal cortex in cataplexy. J Neurosci. 33:9743–9751.
Palomero-Gallagher N, Zilles K. 2004. Isocortex. In: Paxinos G, editor. The rat nervous system. 3rd ed. Amsterdam (The Netherlands): Elsevier Academic Press. pp. 729–753.
Paulussen M, Jacobs S, Van der Gucht E, Hof PR, Arckens L. 2011. Cytoarchitecture of the mouse neocortex revealed by the low-molecular-weight neurofilament protein subunit. Brain Struct Funct. 216:183–199.
Paxinos G, Franklin KBJ. 2001. The mouse brain in stereotaxic coordinates. 2nd ed. San Diego (CA): Academic Press. p. 296.
Peyron C, Faraco J, Rogers W, Ripley B, Overeem S, Charnay Y, Nevsimalova S, Aldrich M, Reynolds D, Albin R et al. 2000. A mutation in a case of early onset narcolepsy and a generalized absence of hypocretin peptides in human narcoleptic brains. Nat Med. 6:991–997.
Peyron C, Tighe DK, van den Pol AN, de Lecea L, Heller HC, Sutcliffe JG, Kilduff TS. 1998. Neurons containing hypocretin (orexin) project to multiple neuronal systems. J Neurosci. 18:9996–10015.
Porter JT, Cauli B, Tsuzuki K, Lambolez B, Rossier J, Audinat E. 1999. Selective excitation of subtypes of neocortical interneurons by nicotinic receptors. J Neurosci. 19:5228–5235.
Richardson KA, Fanselow EE, Connors BW, 2007. Neocortical anatomy and physiology. In: Engel J Jr, Pedley TA, editors. Epilepsy: a comprehensive textbook. 2nd ed. Philadelphia (PA): Lippincott Williams and Wilkins. p. 323–335.
Rieger M, Mayer G, Gauggel S. 2003. Attention deficits in patients with narcolepsy. Sleep. 26:36–43.
Rudy B, Fishell G, Lee S, Hjerling-Leffler J. 2011. Three groups of interneurons account for nearly 100% of neocortical GABAergic neurons. Dev Neurobiol. 71:45–61.
Sakurai T. 2007. The neural circuit of orexin (hypocretin): maintaining sleep and wakefulness. Nat Rev Neurosci. 8:171–181.
Sakurai T, Amemiya A, Ishii M, Matsuzaki I, Chemelli RM, Tanaka H, Williams SC, Richarson JA, Kozlowski GP, Wilson S et al. 1998. Orexins and orexin receptors: a family of hypothalamic neuropeptides and G protein-coupled receptors that regulate feeding behaviour. Cell. 92:573–585.
Schöne C, Cao ZF, Apergis-Schoute J, Adamantidis A, Sakurai T, Burdakov D. 2012. Optogenetic probing of fast glutamatergic transmission from hypocretin/orexin to histamine neurons in situ. J Neurosci. 32:12437–12443.
Smart D, Jerman JC, Brough SJ, Rushton SL, Murdock PR, Jewitt F, Elshourbagy NA, Ellis CE, Middlemiss DN, Brown F. 1999. Characterization of recombinant human orexin receptor pharmacology in a Chinese hamster ovary cell-line using FLIPR. Br J Pharmacol. 128:1–3.
Smart D, Sabido-David C, Brough SJ, Jewitt F, Johns A, Porter RA, Jerman JC. 2001. SB-334867-A: the first selective orexin-1 receptor antagonist. Br J Pharmacol. 132:1179–1182.
Spinazzi R, Andreis PG, Rossi GP, Nussdorfer GG. 2006. Orexins in the regulation of the hypothalamic-pituitary-adrenal axis. Pharmacol Rev. 58:46–57.
Sutcliffe JG, de Lecea L. 2002. The hypocretins: setting the arousal threshold. Nat Rev Neurosci. 3:339–349.
Thannickal TC, Moore RY, Nienhuis R, Ramanathan L, Gulyani S, Aldrich M, Cornford M, Siegel JM. 2000. Reduced number of hypocretin neurons in human narcolepsy. Neuron. 27:469–474.
Trantham-Davidson H, Kröner S, Seamans JK. 2008. Dopamine modulation of prefrontal cortex interneurons occurs independently of DARPP-32. Cereb Cortex. 18:951–958.

Uylings HB, Groenewegen HJ, Kolb B. 2003. Do rats have a prefrontal cortex? Behav Brain Res. 146:3–17.
Van de Werd HJ, Rajkowska G, Evers P, Uylings HB. 2010. Cytoarchitectonic and chemoarchitectonic characterization of the prefrontal cortical areas in the mouse. Brain Struct Funct. 214:339–353.
Vittoz NM, Berridge CW. 2006. Hypocretin/orexin selectively increases dopamine efflux within the prefrontal cortex: involvement of the ventral tegmental area. Neuropsychopharmacology. 31:384–395.
Xia J, Chen X, Song C, Ye J, Yu Z, Hu Z. 2005. Postsynaptic excitation of prefrontal cortical pyramidal neurons by hypocretin-1/orexin A through the inhibition of potassium currents. J Neurosci Res. 82:729–736.
Yamanaka A, Beuckmann CT, Willie JT, Hara J, Tsujino N, Mieda M, Tominaga M, Yagami KI, Sugiyama F, Goto K et al. 2003. Hypothalamic orexin neurons regulate arousal according to energy balance in mice. Neuron. 38:701–713.
Yamanaka A, Tsujino N, Funahashi H, Honda K, Guan JL, Wang QP, Tominaga M, Goto K, Shioda S, Sakurai T. 2002. Orexins activate histaminergic neurons via the orexin 2 receptor. Biochem Biophys Res Commun. 290:1237–1245.